

**A Mathematical Model on the Effect of Cultural Practices
on HIV Transmission Dynamics in Western Kenya**

Lago, Sally Stella

167902

**Submitted in Partial Fulfillment of the Requirements for the Degree of
Master of Science in Biomathematics at Strathmore University**



**Strathmore Institute of Mathematical Sciences
Strathmore University**

Nairobi, Kenya

June, 2025

This thesis is available for Library use on the understanding that it is copyright material and that no quotation from the thesis may be published without proper acknowledgement.

Declaration and Approval

Declaration

I declare that this work has not been previously submitted and approved for the award of a degree by this or any other University. To the best of my knowledge and belief, the thesis contains no material previously published or written by another person except where due reference is made in the thesis itself.

©No part of this thesis may be reproduced without the permission of the author and Strathmore University.

Student's Name: **Lago Sally Stellah**

Signature: _____  Date: May 22, 2025

Approval

The thesis of **Lago Sally Stellah** was reviewed and approved by the following:

Prof. Rachel Waema Mbogo

Supervisor,

Strathmore Institute of Mathematical Sciences, Strathmore University.

Dr. Titus Orwa

Supervisor,

Strathmore Institute of Mathematical Sciences, Strathmore University.

Dr. Geoffrey Madigu

Dean of Strathmore Institute of Mathematical Sciences

Prof. Bernard Shibwabo

Director of Graduate Studies

Abstract

The HIV epidemic remains one of the most significant global health challenges, with Sub-Saharan Africa, particularly Kenya, facing a substantial burden. The Luo-Nyanza region in Western Kenya, historically a hotspot for HIV infection, consistently reports higher prevalence rates compared to the national average. Moreover, despite the fact that there have been significant progress in the reduction of new HIV infection the counties residing in the Luo-Nyanza region have consistently contributed to a significant number of new infections nationally. It is hypothesized that specific cultural practices, such widow cleansing rituals, wife inheritance and polygamy contribute to the elevated risk of HIV transmission within this community. Thus the study sought to model HIV transmission dynamics in the presence of these predisposing cultural practices. This study developed and utilized a deterministic compartmental model to determine the effects of cultural practices on HIV transmission dynamics in the Luo-Nyanza region of Western Kenya. The effective reproduction number was computed using the next-generation matrix approach, and the system was solved numerically using the fourth-order Runge-Kutta method. Sensitivity analysis of the basic reproduction number revealed that infection rate and cultural practices had the greatest influence on the model's outcomes. Numerical simulations further demonstrated that these cultural practices negatively impact HIV transmission dynamics, affecting both the retention to care and overall disease burden, ultimately leading to higher infection rates. The findings show that when such practices are adversely practiced, the infection rate increases by 42% and dropout rates by 65%. These results highlight the urgent need for culturally tailored interventions such as engaging community elders, integrating HIV education into traditional gatherings, promoting safe alternatives to widow cleansing and wife inheritance, and collaborating with cultural leaders to shift harmful norms. As eradicating these traditions entirely may not be feasible, such targeted interventions offer a pragmatic approach to mitigating their impact.

Table of Contents

Declaration and Approval	ii
List of Figures	vii
List of Tables	viii
List of Abbreviations	ix
Acknowledgement	x
1 Introduction	1
1.1 Background to the Study	1
1.2 Statement of the Problem	4
1.3 Research Objectives	4
1.3.1 General Objective	4
1.3.2 Specific Objectives	5
1.4 Scope of the Study	5
1.5 Significance of the study	5
2 Literature Review	7
2.1 Introduction	7
2.1.1 HIV and Cultural Practices in Luo-Nyanza Region	7
2.1.2 Use of Mathematical Models in Modelling HIV and Culture	8
2.1.3 Current Research	10
3 Methodology	11

3.1	Introduction	11
3.2	Source of Data	11
3.3	Model Description	11
3.4	Model Assumptions	13
3.5	Compartmental Model	14
3.6	Model Equations	16
3.7	Mathematical Analysis of the Model	16
3.7.1	Positivity of Solutions	16
3.7.2	Boundedness of Solutions	20
3.8	Equilibrium States	22
3.8.1	Disease Free Equilibrium Point, DFE	22
3.9	Reproduction Number	23
3.9.1	Effective Reproduction Number (R_v)	23
3.10	Stability Analysis	26
3.10.1	Local Stability of the Disease-free Equilibrium	26
3.10.1.1	Global Stability of the Disease-free Equilibrium	28
3.10.1.2	Endemic Equilibrium Points	29
4	Sensitivity Analysis and Numerical Simulations	31
4.1	Introduction	31
4.1.1	Sensitivity Analysis	31
4.1.2	Numerical Simulations	33
4.1.3	Effect of Cultural Practices on the Effective Reproduction Number	34
4.1.3.1	Effect of Cultural Practices on HIV Infection Dynamics	35
4.1.3.2	Effect of Cultural Practices on Retention to Treatment	36
4.1.3.3	Effect of Cultural Practices on Viral Load Suppression	37
4.1.3.4	Effect of Cultural Practices on ART Treatment	39
5	Conclusion and Recommendation	41
5.1	Recommendation	42
5.2	Future Research	42

References	44
Appendix A	46
Appendix B	48
Appendix C	49
Appendix D	50



List of Figures

Figure 3.1: Non-Parameterized Model diagram for HIV and Culture	15
Figure 3.2: Parameterized Model diagram for HIV and Culture	15
Figure 4.1: A graph showing the effect of cultural practices on the reproduction number	34
Figure 4.2: A graph showing the effect of cultural practices on HIV infection dynamics at Low Cultural Influence: 0.1–0.3, Moderate Cultural Influence: 0.35–0.55, High Cultural Influence: 0.60–0.90.	35
Figure 4.3: A graph showing the effect of cultural practices on retention to Treatment at Low cultural influence: 0.1–0.3, Moderate Cultural Influence: 0.35–0.55, High Cultural Influence: 0.60–0.90.	36
Figure 4.4: A graph showing the effect of cultural practices on viral load suppression at Low cultural influence: 0.1–0.3, Moderate Cultural Influence: 0.35–0.55, High Cultural Influence: 0.60–0.90.	38
Figure 4.5: A graph showing the effect of cultural practices on ART treatment at Low cultural influence: 0.1–0.3, Moderate Cultural Influence: 0.35–0.55, High Cultural Influence: 0.60–0.90.	39

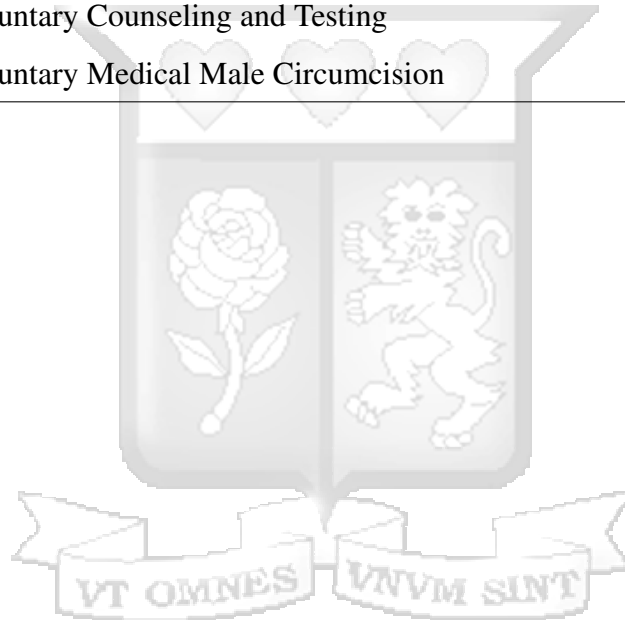
List of Tables

Table 3.1: Table of Model Variables	13
Table 3.2: Model Parameters	14
Table 4.1: Sensitivity Analysis of Parameters.	33



List of Abbreviations

AIDS	Acquired Immunodeficiency Syndrome
ART	Antiretroviral Therapy
HIV	Human Immunodeficiency Virus
NASCOP	National AIDS and STI Control Program
NSDCC	National Syndemic Diseases Control Council
PLWHIV	People Living with HIV
VCT	Voluntary Counseling and Testing
VMMC	Voluntary Medical Male Circumcision



Acknowledgement

First and foremost, I am deeply grateful to God for granting me the strength, resilience, and grace to see this journey through. I would also like to extend my heartfelt gratitude to my supervisors, Dr. Titus Orwa and Professor Rachel Waema, for their dedication, unwavering support and generous investment of time and effort throughout this journey. Thank you for continuously challenging me to think critically, for always making time to review my work and for encouraging me every step of the way. Your guidance and insights have been invaluable to the successful completion of this thesis.

A special thank you to my loving husband, Lenwesley Khendi, for your constant love, support, and patience. Without you, this day would not have been possible. Thank you for staying up with me during the long nights and walking this path by my side. To our daughter, Nimora Khendi your presence has been a beautiful reminder of hope and purpose. Even as a newborn, your peaceful naps gifted me the quiet moments I needed to write and your presence inspired me to keep going with love and determination. I am deeply thankful to my parents, Linet and Willis, for their unwavering support throughout the many years of my studies.

I also wish to thank my dear study mates, Kennedy and Cecilia, for their continuous encouragement, insightful discussions and shared commitment that made this academic journey more enriching and bearable. Finally, I extend my gratitude to everyone who has supported me in one way or another your kindness and encouragement have truly made a difference.

Chapter 1

Introduction

1.1 Background to the Study

Human Immunodeficiency Virus/Acquired Immunodeficiency Syndrome (HIV/AIDS) epidemic is one of the most pressing global health challenges of our time, with Sub-Saharan Africa (SSA) bearing the heaviest burden of the disease ([Kharsany and Karim, 2016](#)). In 2022, over two-thirds of the world's estimated 39 million people living with HIV lived in this region HIV disproportionately affects women and girls accounting for 53% of all HIV cases globally, with 46% of all new infections occurring within this demographic worldwide ([Van Schalkwyk et al., 2024](#)).

HIV is a retrovirus that specifically targets CD4+ T cells, a critical component of the human immune system. HIV weakens the immune system by infecting and gradually destroying CD4+ T cells ([Ngina et al., 2017](#)). The virus binds to specific receptors on the surface of the T cell, gains entry, and integrates its genetic material (RNA) into the host cell's DNA. This allows HIV to attack the cellular machinery to produce new HIV virions. These newly produced viruses are then released from the infected CD4+ T cell, capable of infecting other healthy CD4+ T cells, perpetuating the cycle of the virus replicating itself and destroying the immune system ([Vijayan et al., 2017](#)). When left untreated, HIV infection progressively weakens the immune system, making individuals susceptible to life-threatening opportunistic infections and illnesses. ([Van Schalkwyk et al., 2024](#)). The most common modes of HIV transmission include unprotected coitus (sex) with an infected individual and mother-to-child transmission during pregnancy, birth, or breastfeeding. Other less frequent transmission routes involve receiving a blood transfusion with infected blood or sharing needles or syringes with someone who has HIV ([Gelmon, 2009](#)).

Kenya, like many countries in Sub-Saharan Africa, grapples with significant HIV infection rates and AIDS-related mortality. Despite the advancements made, a concerning disparity exists within the country with the Luo-Nyanza region consistently reporting a disproportionately high HIV prevalence compared to other areas. Historically, the region has been a hotspot for HIV infection. In 2009, the HIV prevalence in Luo-Nyanza was at 14.9%, which was twice as high as the national average and highlighting the region's substantial burden, estimated at 30% of the national total (Gelmon, 2009). The Kenya Population-based HIV Impact Assessment Report 2018 revealed that the Luo-Nyanza region, particularly Homa Bay County, exhibited a significantly higher HIV prevalence compared to the national average. Homa Bay County reported the highest prevalence at 19.6%, a figure four times higher than the national average of 4.9%. Following closely were Kisumu County with 17.5%, Siaya County with 15.3%, and Migori County with 13.0% (Kenya Ministry of Health, 2020). In 2021, the National Syndemic Diseases Control Council report emphasized the disproportionate burden of the HIV epidemic evident in Kenya, where ten counties accounted for 58% (835,803) of the total population living with HIV (PLWHIV) nationwide with notably, five of these counties reported to be in the Luo-Nyanza region (NSDCC, 2022). The most recent report in 2023 reiterated the high HIV prevalence in Luo-Nyanza, with Homa Bay County recording the highest prevalence of 15.2%, followed by Kisumu 14.5%, Siaya 13.2%, and Migori 9.7% (NSDCC, 2023).

It is hypothesized that the region practices unique traditions that predispose it to a higher risk of HIV prevalence (Magadi et al., 2021). Cultural practices such as widow cleansing and wife inheritance and polygamy are thought to contribute to this elevated burden (Munala et al., 2019). Widow cleansing rituals involve a widow engaging in unprotected sexual intercourse with a designated “cleanser”, often a relative. In recent years, however, it has been reported that in-laws have become less willing to participate in this practice. As a result, the practice has been commercialized, with professional inheritors being paid to perform the ritual across different families (Magadi et al., 2021). The practice of widow cleansing is believed to cleanse the widow of any perceived impurity acquired upon her husband's death and allow her deceased husband's spirit to find peace. However, the consequences can be devastating. If the widow is HIV-positive, she can transmit the virus to the cleanser. Conversely, if the

cleanser is infected, the widow faces a high risk of contracting HIV. The case worsens when professional cleansers are employed as this can lead to multiple transmissions to widowed women if either the widow or cleanser is HIV positive.

Wife inheritance, another cultural practice in the region, further complicates the fight against HIV. Under this custom, a widowed woman is expected to be “inherited” by a relative of her deceased husband. This practice can contribute to the spread of HIV if either the widow or the inheriting relative is infected. Closely correlating with widow cleansing and wife inheritance, gender roles in the Luo-Nyanza region have contributed to discriminatory power imbalance towards women. This has consequently affected women’s ability and power in sexual decision-making and access to healthcare services thus conforming to societal norms and increasing their vulnerability to HIV infection.

There are significant medical strides that have been made in HIV prevention and treatment in Luo-Nyanza through various strategies. Antiretroviral Therapy (ART) has been widely implemented in the region. Voluntary Medical Male Circumcision (VMMC) programs have been promoted as a crucial HIV prevention strategy, given the procedure’s ability to reduce the risk of HIV transmission. Voluntary Counseling and Testing (VCT) services are crucial for early detection and treatment of HIV. The efforts to increase awareness and uptake of VCT services have been moderately successful. However, stigma, poverty, and risky cultural behaviors impede this efforts. While much has been done on poverty and stigma, minimal mathematical research have been done to assess the extent to which cultural practices affect the transmission dynamics in the Luo-Nyanza region.

Therefore in response to the complex challenges posed by the HIV/AIDS epidemic, particularly in light of the interplay between cultural practices and treatment outcomes, this study seeks to develop a mathematical model for HIV infection that seeks to accurately capture the intricate dynamics of HIV transmission within the Luo-Nyanza region, a focal point of the epidemic. Unlike other transmission dynamics models, the approach in this study integrates cultural practices prevalent in the region, recognizing their significant influence on HIV infection. Hence this study tries to answer the question: “Do cultural practices bear an influence on HIV transmission dynamics among the Luo-Nyanza community in Kenya?”

1.2 Statement of the Problem

The HIV epidemic continues to pose a significant global health challenge with an estimated 39 million people living with HIV. Kenya, similarly continues to bear a substantial share of this burden, particularly in the Luo-Nyanza region. Despite the fact that there have been significant progress in the reduction of new HIV infection the counties residing in the Luo-Nyanza region have consistently contributed to a significant number of new infections nationally. The Luo-Nyanza region is known for deeply rooted cultural traditions, including widow cleansing (ritual sexual intercourse to "cleanse" a widow following her husband's death), wife inheritance (where a widow is inherited by a male relative of her deceased husband), and polygamy (where a man has multiple spouses). While these practices hold cultural importance, they often involve unprotected sexual activity and occur outside formal healthcare structures, thereby heightening the risk of HIV transmission.

Despite growing awareness of the risks associated with such practices, there is limited quantitative understanding of how these culturally embedded practices influence HIV transmission dynamics at the population level. Thus, to bridge this gap, this study developed and analyzed a mathematical model of HIV transmission dynamics incorporating cultural practices, in order to understand how risky cultural practices contribute to the elevated burden of the HIV epidemic within a community or region.

1.3 Research Objectives

1.3.1 General Objective

The main objective of this study is to develop and analyze a mathematical model for HIV transmission that incorporates the effects of cultural practices and identify effective strategies for reducing HIV transmission in communities with rich predisposing cultural practices.

1.3.2 Specific Objectives

1. To develop a model for HIV infection incorporating cultural practices in Luo-Nyanza region.
2. To conduct mathematical analysis for the formulated model.
3. To investigate how cultural practices impact the transmission dynamics of HIV in the Luo-Nyanza region.

1.4 Scope of the Study

This research focused on developing a compartmental model to analyze the transmission dynamics of HIV in the Luo-Nyanza region. The analysis was carried out using data from the Luo-Nyanza region sourced from the National Syndemic Disease Control Council (NSDCC). The well-posedness of the model was established by demonstrating the positivity of state variables and the boundedness of solutions. The effective reproduction number, R_v was derived using the Next Generation Matrix method. The local and global stability of the disease-free equilibrium were examined. The model parameters were inferred from existing literature and others estimated. The model was then simulated using the Matlab ODE solvers to analyze the transmission dynamics and the effect of different parameters. The study places special attention to the cultural practices predominant in the the Luo-Nyanza regions to quantify their effect on the transmission dynamics.

1.5 Significance of the study

This study developed a mathematical model to assess the impact of cultural practices on HIV transmission. The findings have significant implications for County Health Management Teams, offering evidence-based recommendations to guide the design and implementation of culturally sensitive interventions aimed at reducing the risk of HIV transmission effectively.

Additionally, the findings provide insights on the adverse effects of risky cultural practices on HIV transmission, thus enhancing community awareness and engagement in combating HIV. By highlighting the role cultural practices play in the spread of the virus, the study encourages greater community involvement in creating and adopting interventions that are not only culturally appropriate but also effective in mitigating transmission.

The insights and mathematical model produced by this study can also be valuable to research and disease modeling institutions, like the Kenya Medical Research Institute (KEMRI) and the National Syndemic Disease Control Council (NSDCC). These organizations can utilize the findings to inform their implementation strategies, ultimately benefiting the broader society by advancing HIV prevention and control efforts.



Chapter 2

Literature Review

2.1 Introduction

In this chapter, the literature on existing HIV models is reviewed highlighting the importance of integrating social and cultural factors to enhance the reliability of mathematical models. Additionally, studies that emphasize the significance of these factors are examined, alongside papers that detail key cultural practices specific to the Luo-Nyanza region, which may influence the development of more accurate and context-sensitive HIV models.

2.1.1 HIV and Cultural Practices in Luo-Nyanza Region

Extensive qualitative and quantitative research work has been done to highlight the potential effect of cultural practices on HIV dynamics in Luo-Nyanza. A study by ([Magadi et al., 2021](#)) revealed that individuals in Luo-Nyanza were six times more likely to be HIV positive as compared to their non-Luo counterparts. The results of the study further revealed that the high prevalence of polygamy and low male circumcision prevalence accounted for part of the disproportionate burden of HIV in Luo-Nyanza. The research recommended targeted research into specific factors driving the epidemic in this region.

[Ayikukwei et al. \(2008\)](#) carried out a study to assess the role of sexual rituals in HIV transmission. The research explored the role of sexual cleansing rituals in the Luo community, revealing how these rituals contribute to the transmission of HIV. The findings underscore the importance of integrating cultural practices like sexual cleansing rituals into mathematical models to capture their impact on sexual behaviors and HIV transmission accurately.

[Agot et al. \(2010\)](#) conducted the first epidemiological study to investigate the association between HIV acquisition and widowhood inheritance. Their results revealed that 63% of widows in their sample were HIV positive and a significant number 53% participated in widow inheritance. The study also highlighted that despite the high risk caused by this practice the population in Bondo district in the Luo-Nyanza were reluctant to stop such practices. The study highlighted that widow inheritance is often sustained not merely as a cultural obligation, but also due to the absence of alternative economic support for widows, in the Luo-Nyanza patrilineal communities where women are not permitted to inherit property, being inherited offers access to housing, land, food, and social acceptance. The lack of formal social protection systems and limited economic opportunities for widowed women further entrenches their dependence on such practices, making it challenging to abandon them despite the well-documented health risks. While their studies showed that widows inherited by professional cleansers were more likely to be infected with HIV as compared to uninherited widows, the study did not reveal the extent to which such practices affected HIV transmission, suggesting a need for further investigation using mathematical models. [Munala et al. \(2019\)](#) expanded on this by exploring the lived experiences of widows who have undergone sexual cleansing rituals, revealing the pervasive violence and lack of consent associated with these practices. Their findings emphasized the intersection of cultural practices, gender-based violence, and HIV transmission, suggesting that cultural norms can serve as both protective factors and risk factors for HIV.

The studies reviewed underscore the potential risk posed by cultural practices specific to the Luo-Nyanza region, highlighting the need for a mathematical approach to assess their impact on HIV dynamics.

2.1.2 Use of Mathematical Models in Modelling HIV and Culture

Mathematical models have been used extensively to understand HIV disease dynamics, predict disease progression, evaluate intervention strategies and control transmission. In 2016, [Huo et al. \(2016\)](#) developed a simple HIV epidemic model with treatment. The model

consisted of the susceptible, infected individuals, those on treatment, those who had full-blown AIDS and those who had changed their sexual behaviors making them immune to HIV infection by sexual contact. The study's finding indicated that increasing the rate of treatment significantly reduces the reproduction number R_0 to less than 1 implying that the disease is eradicated. The model, however, did not account for the effect of different demographics on the transmission dynamics. [Mwangi et al. \(2024\)](#) utilized a simple SIAT (Susceptible-Infected-full blown AIDS-Treatment) model. The findings of the study revealed that when the treatment rate of those infected increases, it leads to an increase in the population on treatment and as a result slows down the spread of the disease.

[Bozkurt and Peker \(2014\)](#) developed a simple HIV model that took into consideration the population of infected individuals who are unaware that they are infected. The study revealed that the spread of the disease decreased as more of the infected population became aware of their HIV status. Conversely, the disease spread increased as the infected people continued to spread the disease due to the unawareness of their status. The research recommended screening and contact tracing of individuals as effective measures to curb the spread of HIV. The introduction of the unaware infectives in the model provided insights into how one's awareness of HIV status significantly impacts the dynamics of the disease.

[Nhendo \(2019\)](#) carried out a study to model the effects of treatment failure on the dynamics of HIV. The research considered the SIR (Susceptible-Infected-Recovered) population. The numerical simulations revealed that increased treatment dropouts led to more transmissions in the population. The study further demonstrated that even with enrollment in Antiretroviral Treatment and a controlled number of dropouts the reproduction number remained above one, implying that these measures alone were insufficient to reduce the spread of the disease. Other treatment strategies are needed to reduce infection. This study provides a foundation for modeling other factors that impact HIV transmission dynamics.

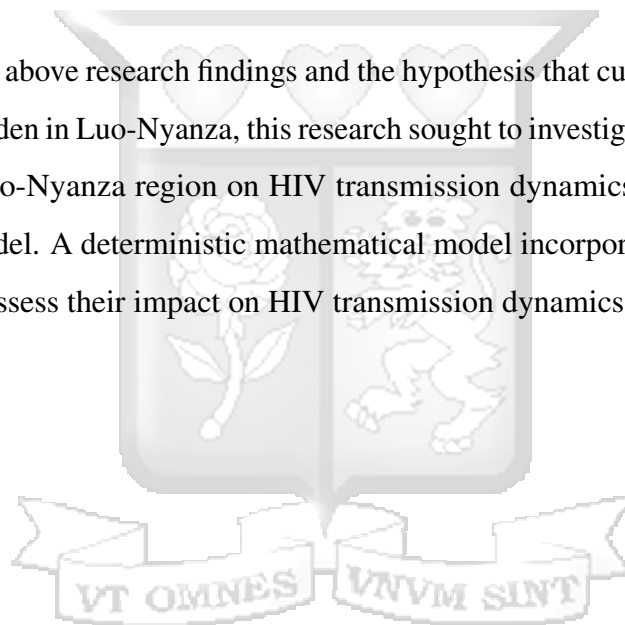
[Udofia \(2023\)](#) conducted a study to model the effect of male circumcision as an HIV prevention method. The study incorporated susceptible individuals both uncircumcised and circumcised, and uncircumcised and circumcised infected individuals. The analysis of the model revealed that if the rate of circumcision is increased while those of disease-induced

death and natural death are reduced this would bring the reproduction number to less than 1 and thus the disease dying out. This study highlighted the importance of introducing male circumcision to mathematical models as a possible prevention strategy.

[Cassels et al. \(2008\)](#) conducted a study that revealed societal context plays a key role in influencing individual behavior and HIV outcomes at the population levels. The study revealed that with the inclusion of societal contexts, mathematical modelling can be used to understand the disparities in the burden of HIV.

2.1.3 Current Research

Thus, in light of the above research findings and the hypothesis that cultural factors contribute to the high HIV burden in Luo-Nyanza, this research sought to investigate the effect of cultural practices in the Luo-Nyanza region on HIV transmission dynamics using a deterministic compartmental model. A deterministic mathematical model incorporating cultural practices was developed to assess their impact on HIV transmission dynamics.



Chapter 3

Methodology

3.1 Introduction

This chapter outlines the methodology employed in this research. The research design is presented under the following sections: model formulation, model flowchart, model assumptions, variables and parameters, and the analytical and numerical methods used for model analysis

3.2 Source of Data

The study utilized epidemiological data derived from the National Syndemic Diseases Control Council (NSDCC) and the Kenya Bureau of Statistics (KNBS). Model parameters were inferred from published studies, while others were appropriately assumed. These parameters were then applied to simulate various scenarios, enabling a comprehensive analysis of the impact of cultural practices on HIV transmission dynamic

3.3 Model Description

The deterministic model in this study utilized five compartments to represent the interplay between HIV transmission dynamics and specific cultural practices like polygamy, wife inheritance, widow cleansing, and male circumcision, which are postulated to play a significant role in facilitating the spread of HIV/AIDS.

The population is divided into Susceptibles (S), individuals infected with HIV (I). Additionally, There are individuals under treatment for HIV (T). Some individuals under treatment achieve significant viral load suppression to undetectable levels (V). Finally, there are individuals who despite being diagnosed and starting treatment, have discontinued their treatment due to factors such as ostracization or cultural beliefs (D) that discourage treatment adherence. Thus, the expression for the total population (N) at any time t is:

$$N(t) = S(t) + I(t) + T(t) + V(t) + D(t).$$

The model assumes the susceptible individuals are recruited at a constant rate Λ (natural birth). The susceptible, acquire HIV positive status following contact with individuals with HIV/AIDS at the rate λ . The transmission rate λ in the Luo-Nyanza region is influenced by cultural practices such as widow cleansing, wife inheritance, and polygamy, which increase exposure to HIV. The function λ can be expressed as:

$$\lambda(t) = \beta \frac{\pi_0 I(t) + \pi_1 D(t)}{N(t)} (1 - \psi_m) \psi_c,$$

where;

$$\psi_c = 1 - [(1 - \alpha_i)(1 - \alpha_w)(1 - \alpha_p)],$$

$0 < \psi_m, \psi_c < 1$ and β is the base infection rate. π_0 and π_1 where $\pi_0 > \pi_1$ are the modification parameter that measures the relative infectiousness of individuals in $I(t)$ compared to individuals in $D(t)$. ψ_m is a parameter that takes into account the reduction in transmission rate due to male circumcision, ψ_c is a parameter that accounts for the increase in transmission due to the negative cultural practices (such as wife inheritance, widow cleansing and polygamy) carried out in the Luo-Nyanza region. The parameters $\alpha_w, \alpha_i, \alpha_p$ are cultural influence factors for widow cleansing, wife inheritance, and polygamy, respectively. Those in class I get enrolled into treatment upon becoming aware of their status at the rate θ_1 . The infected individuals receiving treatment can drop out of treatment due to cultural beliefs and societal pressure at the rate of θ_2 . Finally, individuals who adhere to treatment can

significantly suppress the viral load to undetectable levels at the rate κ . These individuals V can drop out of treatment due to cultural beliefs and societal pressure at the rate of θ_2

3.4 Model Assumptions

1. The susceptible individuals can only contract a disease at a time
2. All individuals who are aware of their HIV status through testing are enrolled in treatment
3. All individuals on treatment not only received ART but also counseling against risky sexual behaviors and as a result do not spread the infection
4. All individuals who do not adhere to treatment drop out of care
5. Infected Individuals who have never been on treatment are relatively more infectious compared to those who dropped out of treatment

The model variables and parameters are as presented in (3.1) and (3.2)

Table 3.1: Table of Model Variables

Symbol	Description
S	Susceptible population
I	Individuals infected with HIV
T	HIV Infected individuals under treatment
V	Individuals with undetectable viral load
D	Individuals who have dropped out from treatment

Table 3.2: Model Parameters

Parameter	Description	Value	Source
Λ	Recruitment rate of susceptible individuals	0.2442	World Bank Estimate 2021
β	HIV infection rate	0.13	NSDCC report 2023
θ_1	Rate of initiation to treatment	0.0094	Nhendo (2019)
θ_2	Rate of non-adherence to treatment	0.039	NSDCC HIV Estimates 2024
π_o	Relative HIV infectiousness of infected	2.2	Assumed
π_1	Relative HIV infectiousness of dropouts	1.8	Assumed
θ_3	Rate of treatment re-initiation of dropouts	0.00902	Nhendo (2019)
κ	Rate of adherence to treatment	0.906	KENPHIA
ψ_m	Protective effect of circumcision	0.5	KENPHIA
α_i	Relative effect of wife inheritance	0.1-0.9	Assumed
α_p	Relative effect of polygamy	0.1-0.9	Assumed
α_w	Relative effect of widow cleansing	0.1-0.9	Assumed
δ	Disease-induced death rate	0.015714286	NACC estimates 2021
μ	Natural death rate	0.00783	World Bank

3.5 Compartmental Model

To provide a comprehensive understanding of the system dynamics, the subsequent page presents the non-paramaterized and parametrized compartmental model diagram along with the governing mathematical equations.

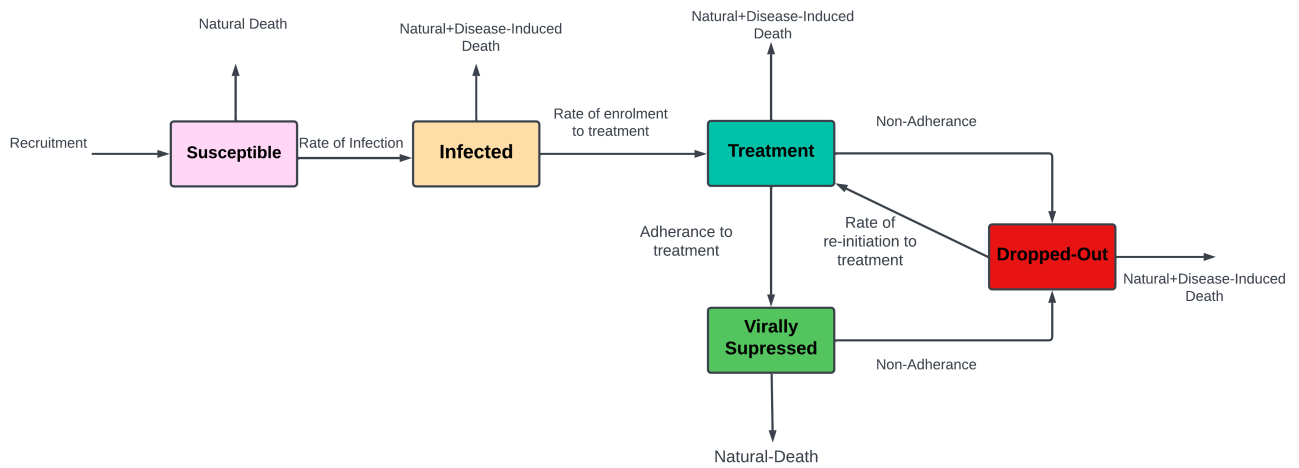


Figure 3.1: Non-Parameterized Model diagram for HIV and Culture

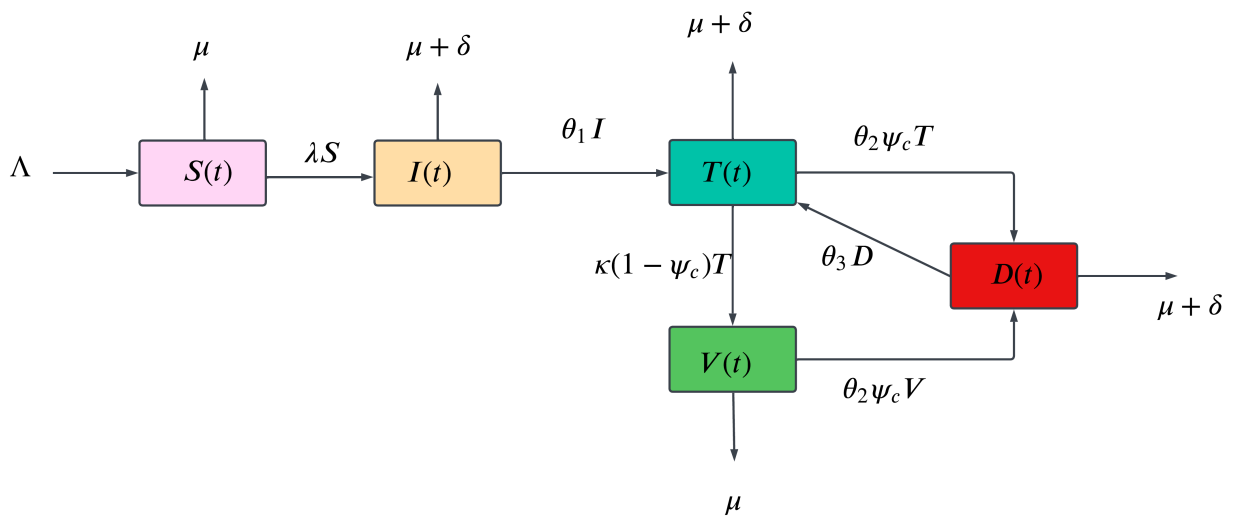


Figure 3.2: Parameterized Model diagram for HIV and Culture

3.6 Model Equations

$$\begin{aligned}\frac{dS(t)}{dt} &= \Lambda - (\lambda + \mu)S, \\ \frac{dI(t)}{dt} &= \lambda S - (\theta_1 + \mu + \delta)I, \\ \frac{dT(t)}{dt} &= \theta_1 I + \theta_3 D - (\theta_2 \psi_c + \kappa(1 - \psi_c) + \mu + \delta)T, \\ \frac{dV(t)}{dt} &= \kappa(1 - \psi_c)T - (\theta_2 \psi_c + \mu)V, \\ \frac{dD(t)}{dt} &= \theta_2 \psi_c(T + V) - (\theta_3 + \mu + \delta)D.\end{aligned}\tag{3.1}$$

With initial conditions

$$S(0) > 0, \quad I(0) \geq 0, \quad T(0) \geq 0, \quad V(0) \geq 0, \quad D(0) \geq 0.$$

3.7 Mathematical Analysis of the Model

3.7.1 Positivity of Solutions

The monitoring of human populations in the model underscores the importance of verifying the non-negativity of its state variables. To clarify, we demonstrate that under initial conditions where all values are non-negative, the solutions to the model will maintain non-negativity for all times $t \geq 0$. This leads us to present the following theorem.

Theorem 3.3.1. *Let the parameters for the model be non-negative constants. A non-negative solution $(S(t), I(t), T(t), V(t), D(t))$ for the model exists for all state variables with initial conditions $(S(t) \geq 0, I(t) \geq 0, T(t) \geq 0, V(t) \geq 0, D(t) \geq 0)$ for all $t \geq 0$.*

Proof. From the first equation of model (3.1)

$$\frac{dS}{dt} = \Lambda - (\lambda + \mu)S.\tag{3.2}$$

Separating the variables we have

$$\frac{dS}{S} \geq -(\lambda + \mu)dt. \quad (3.3)$$

Integrating (3.3) gives

$$\ln S \geq -\left(\int_0^t (\lambda + \mu)dt\right) + C_1. \quad (3.4)$$

Taking exponents on both sides we obtain

$$S \geq C_2 \exp\left(-\int_0^t (\lambda + \mu)dt\right). \quad (3.5)$$

Taking the initial conditions at $t = 0$ and $S(0) = S_0$, then from (3.5) we have $C_2 = S_0$.

Equation (3.5) can be re-written as

$$S \geq S_0 \exp\left(-\int_0^t (\lambda + \mu)dt\right). \quad (3.6)$$

As $t \rightarrow \infty$, $S(t) \geq 0$, $\forall t \geq 0$.

From the second equation of model (3.1)

$$\frac{dI}{dt} = \lambda S - (\theta_1 + \mu + \delta)I. \quad (3.7)$$

Separating the variables we have

$$\frac{dI}{I} \geq -(\theta_1 + \mu + \delta)dt. \quad (3.8)$$

Integrating (3.8) gives

$$\ln I \geq - \left(\int_0^t -(\theta_1 + \mu + \delta) dt \right) + C_1. \quad (3.9)$$

Taking exponents on both sides we obtain

$$I \geq C_2 \exp(-(\theta_1 + \mu + \delta)t). \quad (3.10)$$

Taking the initial conditions at $t = 0$ and $I(0) = I_0$, then from (3.10) we have $C_2 = I_0$.

Equation (3.10) can be re-written as

$$I \geq I_0 \exp(-(\theta_1 + \mu + \delta)t). \quad (3.11)$$

As $t \rightarrow \infty$, $I(t) \geq 0$, $\forall t \geq 0$.

From the third equation of model (3.1)

$$\frac{dT}{dt} = \theta_1 I - (\theta_2 \psi_c + \kappa(1 - \psi_c) + \mu + \delta)T. \quad (3.12)$$

Separating the variables we have

$$\frac{dT}{T} \geq -(\theta_2 \psi_c + \kappa(1 - \psi_c) + \mu + \delta)dt. \quad (3.13)$$

Integrating (3.13) gives

$$\ln T \geq - \left(\int_0^t -(\theta_2 \psi_c + \kappa(1 - \psi_c) + \mu + \delta) dt \right) + C_1. \quad (3.14)$$

Taking exponents on both sides we obtain

$$T \geq C_2 \exp(-(\theta_2 \psi_c + \kappa(1 - \psi_c) + \mu + \delta)t). \quad (3.15)$$

Taking the initial conditions at $t = 0$ and $T(0) = T_0$, then from (3.15) we have $C_2 = T_0$.

Equation (3.15) can be re-written as

$$T \geq T_0 \exp(-(\theta_2 \psi_c + \kappa(1 - \psi_c) + \mu + \delta)t). \quad (3.16)$$

As $t \rightarrow \infty$, $T(t) \geq 0$, $\forall t \geq 0$.

From the fourth equation of model (3.1)

$$\frac{dV}{dt} = \kappa(1 - \psi_c)T - (\theta_2 \psi_c + \mu)V. \quad (3.17)$$

Separating the variables we have

$$\frac{dV}{V} \geq -(\theta_2 \psi_c + \mu)dt. \quad (3.18)$$

Integrating (3.18) gives

$$\ln V \geq -\left(\int_0^t -(\theta_2 \psi_c + \mu) dt\right) + C_1. \quad (3.19)$$

Taking exponents on both sides we obtain

$$V \geq C_2 \exp(-(\theta_2 \psi_c + \mu)t). \quad (3.20)$$

Taking the initial conditions at $t = 0$ and $V(0) = V_0$, then from (3.20) we have $C_2 = V_0$.

Equation (3.20) can be re-written as

$$V \geq V_0 \exp(-(\theta_2 \psi_c + \mu)t). \quad (3.21)$$

As $t \rightarrow \infty$, $V(t) \geq 0$, $\forall t \geq 0$.

From the fifth equation of model (3.1)

$$\frac{dD}{dt} = \theta_2 \psi_c(T + V) - (\theta_3 + \mu + \delta)D. \quad (3.22)$$

Separating the variables we have

$$\frac{dD}{D} \geq -(\theta_3 + \mu + \delta)dt. \quad (3.23)$$

Integrating (3.23) gives

$$\ln D \geq -\left(\int_0^t -(\theta_3 + \mu + \delta)dt\right) + C_1. \quad (3.24)$$

Taking exponents on both sides we obtain

$$D \geq C_2 \exp(-(\theta_3 + \mu + \delta)t). \quad (3.25)$$

Taking the initial conditions at $t = 0$ and $D(0) = D_0$, then from (3.25) we have $C_2 = D_0$.

Equation (3.25) can be re-written as

$$D \geq D_0 \exp(-(\theta_3 + \mu + \delta)t). \quad (3.26)$$

As $t \rightarrow \infty$, $D(t) \geq 0$, $\forall t \geq 0$.

It has been shown that all the state variables $(S(t), I(t), T(t), V(t), D(t))$ are non-negative for all $t \geq 0$. Therefore, the solutions of our system remain non-negative for all $t \geq 0$.

3.7.2 Boundedness of Solutions

Theorem 3.3.2 All solutions $(S(t), I(t), T(t), V(t), D(t)) \in \mathbb{R}^5$ are bounded.

Proof. The total population N at any time t is

$$N(t) = S(t) + I(t) + T(t) + V(t) + D(t).$$

Therefore,

$$\frac{dN}{dt} = \frac{d}{dt} [S(t) + I(t) + T(t) + V(t) + D(t)]. \quad (3.27)$$

$$\frac{dN}{dt} = \frac{d}{dt} [\Lambda - \mu N - \delta(I + T + D)]. \quad (3.28)$$

When there is no infection in the population, there is no death due to the infection, and hence $\delta = 0$

$$\frac{dN}{dt} \leq \Lambda - \mu N. \quad (3.29)$$

Rearranging we have

$$\frac{dN}{dt} + \mu N = \Lambda. \quad (3.30)$$

The integrating factor for (3.30) is $e^{\mu t}$. Multiplying (3.30) by integrating factor gives

$$\frac{dN}{dt} e^{\mu t} + e^{\mu t} \mu N \leq \Lambda e^{\mu t}, \quad (3.31)$$

$$\frac{d}{dt} [N e^{\mu t}] \leq \Lambda e^{\mu t}. \quad (3.32)$$

On integrating (3.32) we get

$$N e^{\mu t} \leq \frac{\Lambda}{\mu} e^{\mu t} + c, \quad (3.33)$$

which simplifies to

$$N \leq \frac{\Lambda}{\mu} + c e^{-\mu t}. \quad (3.34)$$

Applying the initial condition in (3.34) i.e, at $t = 0, N = N(0) = N_0$ we obtain,

$$N_0 = \frac{\Lambda}{\mu} + c \quad \text{and} \quad c = N_0 - \frac{\Lambda}{\mu}. \quad (3.35)$$

Hence,

$$N(t) \leq \frac{\Lambda}{\mu} + (N_0 - \frac{\Lambda}{\mu})e^{-\mu t}. \quad (3.36)$$

As $t \rightarrow \infty$ (3.36) becomes

$$N(t) \leq \frac{\Lambda}{\mu}, \quad (3.37)$$

which can be written as

$$\lim_{t \rightarrow \infty} N(t) \leq \frac{\Lambda}{\mu} \quad (3.38)$$

called the upper bound. Thus, $0 \leq N(t) \leq \frac{\Lambda}{\mu}$.

From equation (3.36) The solution to the model is bounded, and the human population remains in the region:

$$\Omega = \{(S, I, T, V, D) \in \mathbb{R}_+^5\}.$$

3.8 Equilibrium States

3.8.1 Disease Free Equilibrium Point, DFE

This is the point at which there is no infection. This equilibrium is given by $I = T = V = D = 0$. Substituting $S = S^0, I = I^0 = 0, T = T^0 = 0, V = V^0 = 0, D = D^0 = 0$ into the system (3.1) yields $\frac{\Lambda}{\mu}$.

Therefore, the disease-free equilibrium points is given by :

$$E^o = (S^o, I^o, T^o, V^o, D^o) = \left(\frac{\Lambda}{\mu}, 0, 0, 0, 0 \right).$$

3.9 Reproduction Number

3.9.1 Effective Reproduction Number (R_v)

The basic reproduction number is defined as the average number of secondary infections produced when one infected individual is introduced into a host population where everyone is susceptible (Diekmann et al., 1990). In the context of this study, R_v characterizes the mean number of secondary HIV infections arising from a single HIV-infected person in the presence of ARV's. It serves as a critical threshold, enabling researchers to gauge the potential persistence or extinction of the disease within a population, thus facilitating projections of future disease dynamics and informed planning. A value of R_v above the threshold i.e., $R_v > 1$ indicates that each infected individual will, on average, transmit the disease to more than one susceptible individual, leading to its spread within the population. Conversely, if R_v falls below the threshold $R_v < 1$, it suggests that each infected individual will, on average, transmit the disease to fewer than one susceptible individual during their infectious period, thus the disease will die out over time. The determination of R_v in this study employs the next-generation matrix method proposed by Van den Driessche & Watmough (2002). R_v is given by $R_v = \rho(FV^{-1})$ where ρ is the spectral radius of the next generation matrix FV^{-1} . F represents the matrix of new infections while V is the rate of transmissions of the infections into and out of the compartments. We consider the classes I , and D to contribute to new infections and hence the subsystem:

$$\begin{aligned}\frac{dI(t)}{dt} &= \lambda S - (\theta_1 + \mu + \delta)I, \\ \frac{dT(t)}{dt} &= \theta_1 I + \theta_3 D - (\theta_2 \psi_c + \kappa(1 - \psi_c) + \mu + \delta)T, \\ \frac{dD(t)}{dt} &= \theta_2 \psi_c (T + V) - (\theta_3 + \mu + \delta)D, \\ \frac{dV(t)}{dt} &= \kappa(1 - \psi_c)T - (\theta_2 \psi_c + \mu)V.\end{aligned}\tag{3.39}$$

From this, the matrix of new infection becomes:

$$F = \begin{bmatrix} \lambda S \\ 0 \\ 0 \\ 0 \end{bmatrix} = \begin{bmatrix} \frac{\beta S(\pi_0 I + \pi_1 D)(1 - [(1 - \alpha_1)(1 - \alpha_2)(1 - \alpha_3)])(1 - \psi_m)}{N} \\ 0 \\ 0 \\ 0 \end{bmatrix}. \quad (3.40)$$

The Jacobian of the matrix F at disease-free equilibrium point (E^o) is

$$F_{E^o} = \begin{bmatrix} \beta \pi_0 (1 - (1 - \alpha_i)(1 - \alpha_p)(1 - \alpha_w))(1 - \psi_m) & \beta \pi_1 (1 - (1 - \alpha_i)(1 - \alpha_p)(1 - \alpha_w))(1 - \psi_m) & 0 & 0 \\ 0 & 0 & 0 & 0 \\ 0 & 0 & 0 & 0 \\ 0 & 0 & 0 & 0 \end{bmatrix}, \quad (3.41)$$

$$F_{E^o} = \begin{bmatrix} p_1 & p_2 & 0 & 0 \\ 0 & 0 & 0 & 0 \\ 0 & 0 & 0 & 0 \\ 0 & 0 & 0 & 0 \end{bmatrix}, \quad (3.42)$$

where

$$p_1 = \beta \pi_0 (1 - (1 - \alpha_i)(1 - \alpha_p)(1 - \alpha_w))(1 - \psi_m),$$

$$p_2 = \beta \pi_1 (1 - (1 - \alpha_i)(1 - \alpha_p)(1 - \alpha_w))(1 - \psi_m).$$

Also the matrix V is given as :

$$V = \begin{bmatrix} (\theta_1 + \mu + \delta)I \\ -\theta_2(1 - (1 - \alpha_i)(1 - \alpha_p)(1 - \alpha_w))(T + V) + (\theta_3 + \mu + \delta)D \\ -\theta_1 - \theta_3 + (\theta_2\psi_c + \kappa(1 - \psi_c) + \mu + \delta)T \\ -\kappa(1 - \psi_c)T + (\theta_2\psi_c + \mu)V \end{bmatrix}. \quad (3.43)$$

At E^o we have

$$V_{E^o} = \begin{bmatrix} \delta + \theta_1 + \mu & 0 & 0 & 0 \\ 0 & \delta + \theta_3 + \mu & -n\psi_c & -n\psi_c \\ -\theta_1 & -\theta_3 & \kappa(1 - \psi_c) + n\psi_c + \delta + \mu & 0 \\ 0 & 0 & -\kappa(1 - \psi_c) & n\psi_c + \mu \end{bmatrix}. \quad (3.44)$$

Thus the Next-generation matrix FV^{-1} is given by:

$$FV^{-1} = \begin{bmatrix} Z_1 & Z_2 & 0 & 0 \\ 0 & 0 & 0 & 0 \\ 0 & 0 & 0 & 0 \\ 0 & 0 & 0 & 0 \end{bmatrix}, \quad (3.45)$$

Where

$$Z_1 = \frac{\beta\pi_0(1 - \psi_m)(1 - (1 - \alpha_i)(1 - \alpha_p)(1 - \alpha_w))}{(\theta_1 + \mu + \delta)},$$

$$Z_2 = \frac{\beta\pi_1(1 - \psi_m)(1 - (1 - \alpha_i)(1 - \alpha_p)(1 - \alpha_w))}{(\theta_3 + \mu + \delta)}.$$

To find the eigenvalues of the matrix (3.45) we solve for FV^{-1} thus the eigenvalues obtained are $\lambda_1 = 0, \lambda_2 = 0, \lambda_3 = 0$ and $\lambda_4 = \frac{\beta\pi_0(1 - \psi_m)(1 - (1 - \alpha_i)(1 - \alpha_p)(1 - \alpha_w))}{\theta_1 + \mu + \delta}$.

Clearly, the spectral radius of FV^{-1} i.e., the largest eigen value is $\frac{\beta\pi_0(1 - \psi_m)(1 - (1 - \alpha_i)(1 - \alpha_p)(1 - \alpha_w))}{(\theta_1 + \mu + \delta)}$.

Therefore, the reproduction number R_v becomes:

$$R_v = \frac{\beta \pi_0 (1 - \psi_m) (1 - (1 - \alpha_i) (1 - \alpha_p) (1 - \alpha_w))}{(\theta_1 + \mu + \delta)}. \quad (3.46)$$

Which is the sum of the expected number of secondary infections generated by a single individual in I and D compartments respectively, each weighted by their infectiousness and average time spent in that state.

The effective reproduction number, R_v , serves as a threshold parameter: if $R_v < 1$, the disease will eventually die out in the population. However, if $R_v > 1$, the steady state E^0 becomes unstable, and the disease persists within the population.

3.10 Stability Analysis

3.10.1 Local Stability of the Disease-free Equilibrium

Theorem 3.3.2 The disease-free equilibrium of the ODE system (3.1) is locally asymptotically stable whenever $R_v < 1$, and unstable if $R_v > 1$, provided that all parameters are positive.

Proof. The local stability of the HIV-culture model at the disease-free equilibrium point

$$E^o = (S^o, I^o, T^o, V^o, D^o).$$

is determined by evaluating the eigenvalues of the Jacobian matrix of the system at E^o . If all eigenvalues are negative when $R_v < 1$, then E^o is locally asymptotically stable. Conversely, if any eigenvalue is positive when $R_v > 1$, E^o becomes unstable.

The Jacobian matrix for our system of equations (3.1) is given by

$$J = \begin{bmatrix} -\frac{\beta \psi_c(1-\psi_m)(D\pi_1+I\pi_o)}{N} - \mu & -\frac{\beta S\pi_o \psi_c(1-\psi_m)}{N} & 0 & 0 & -\frac{\beta S\pi_1 \psi_c(1-\psi_m)}{N} \\ \frac{\beta \psi_c(1-\psi_m)(D\pi_1+I\pi_o)}{N} & -\delta - \theta_1 - \mu + \frac{\beta S\pi_o \psi_c(1-\psi_m)}{N} & 0 & 0 & \frac{\beta S\pi_1 \psi_c(1-\psi_m)}{N} \\ 0 & \theta_1 & -\delta - \theta_2 \psi_c - \kappa(1-\psi_c) - \mu & 0 & \theta_3 \\ 0 & 0 & \kappa(1-\psi_c) & -\theta_2 \psi_c - \mu & 0 \\ 0 & 0 & \theta_2 \psi_c & \theta_2 \psi_c & -\delta - \theta_3 - \mu \end{bmatrix} \quad (3.47)$$

The Jacobian is well-posed since the additions at each column equals the removal rates from each compartment. The Jacobian matrix at disease-free equilibrium E_o can be written as:

$$J = \begin{bmatrix} -\mu & -\beta \pi_o \psi_c(1-\psi_m) & 0 & 0 & -\beta \pi_1 \psi_c(1-\psi_m) \\ 0 & \beta \pi_o \psi_c(1-\psi_m) - \delta - \theta_1 - \mu & 0 & 0 & \beta \pi_1 \psi_c(1-\psi_m) \\ 0 & \theta_1 & -\delta - \theta_2 \psi_c - \kappa(1-\psi_c) - \mu & 0 & \theta_3 \\ 0 & 0 & \kappa(1-\psi_c) & -\theta_2 \psi_c - \mu & 0 \\ 0 & 0 & \theta_2 \psi_c & \theta_2 \psi_c & -\delta - \theta_3 - \mu \end{bmatrix}. \quad (3.48)$$

The eigenvalues of the characteristic polynomial of the Jacobian matrix are:

$$\lambda_1 = -\mu, \lambda_2 = -\delta - \theta_3 - \mu, \lambda_3 = -\theta_2 \psi_c - \mu, \lambda_4 = -\delta - \theta_2 \psi_c - \kappa(1 - \psi_c) - \mu, \\ \lambda_5 = \beta \pi_o \psi_c(1 - \psi_m) - \delta - \theta_1 - \mu.$$

λ_5 can be further written as:

$$\lambda_5 = -(\delta + \theta_1 + \mu) \left(1 - \frac{\beta \pi_o(1 - \psi_m) \psi_c}{(\delta + \theta_1 + \mu)} \right), \quad (3.49)$$

whereby $\frac{\beta \pi_o(1 - \psi_m) \psi_c}{\delta + \theta_1 + \mu}$ is a threshold value, thus λ_5 can be rewritten as

$$\lambda_5 = -(\delta + \theta_1 + \mu)(1 - R_v). \quad (3.50)$$

Therefore, it follows that λ_5 will be negative provided that $R_v < 1$. If this is true, it implies that all eigenvalues will be less than 1 implying local stability of the system.

3.10.1.1 Global Stability of the Disease-free Equilibrium

Theorem 3.3.3 The Disease Free Equilibrium E^0 of a system is globally asymptotically stable provided that $R_v < 1$.

Proof. The global stability of the disease-free equilibrium is studied using the Lyapunov stability theorem which investigates the existence of a function V such that $V : R^n \rightarrow R$ satisfies

- $V(x^*) = 0$ when $x = x^*$ at steady state,
- $V(x) \geq 0$ for $x \neq x^*$,
- $\dot{V}(x) \leq 0 \forall x$.

From the system of equation we form the function $V = aI + bD$.

It can clearly be shown that at steady state $V(I, D) = 0$ and the $V(I, D) > 0 \forall (I, D) \neq 0$.

To prove the third property we have

$$\frac{dv}{dt} = a \left[\frac{\beta S \psi_c (1 - \psi_m) (\pi_0 I + \pi_1 D)}{N} - (\delta + \theta_1 + \mu) I \right] + b [\theta_2 \psi_c (T + V) - (\delta + \theta_3 + \mu) D], \quad (3.51)$$

This can be rewritten as:

$$\begin{aligned} \frac{dv}{dt} \leq a \left[\frac{\beta \Lambda \psi_c (1 - \psi_m) \pi_0 I}{\mu N} + \frac{\beta \Lambda \psi_c (1 - \psi_m) \pi_1 D}{\mu N} - (\theta_1 + \mu + \delta) I \right] \\ + b [\theta_2 \psi_c (T + V)] - b [(\delta + \theta_3 + \mu) D], \end{aligned} \quad (3.52)$$

Grouping the like-terms together:

$$\begin{aligned} \frac{dv}{dt} \leq a \left[\frac{\beta \Lambda \psi_c (1 - \psi_m) \pi_0}{\mu N} - (\theta_1 + \mu + \delta) \right] I \\ + \left[a \frac{\beta \Lambda \psi_c (1 - \psi_m) \pi_1}{\mu N} - b(\delta + \theta_3 + \mu) \right] D \\ + b [\theta_2 \psi_c (T + V)]. \end{aligned} \quad (3.53)$$

Say the value of $a = 1$ and setting all other classes other than the most infectious class I to zero we have:

$$\frac{dv}{dt} \leq \left[\frac{\beta \psi_c \Lambda (1 - \psi_m) \pi_0}{\mu N} - (\theta_1 + \mu + \delta) \right] I, \quad (3.54)$$

which can be written in terms of R_v and on simplifying, we have:

$$\frac{dv}{dt} \leq \frac{\Lambda}{\mu N} \left[\frac{\beta \psi_c (1 - \psi_m) \pi_0}{(\theta_1 + \mu + \delta)} - 1 \right] I, \quad (3.55)$$

$$\frac{dv}{dt} \leq \left[\frac{\beta \Lambda (1 - \psi_m) \pi_0}{\mu N (1 - \psi_c)} - (\theta_1 + \mu + \delta) \right] I, \quad (3.56)$$

$$\frac{dv}{dt} \leq \left[\frac{\beta \psi_c \Lambda (1 - \psi_m) \pi_0}{\mu N ((\theta_1 + \mu + \delta))} - 1 \right] I, \quad (3.57)$$

which can be rewritten as:

$$\frac{dv}{dt} \leq \frac{\Lambda}{\mu N} [R_v - 1] I. \quad (3.58)$$

If $R_v < 1$ the $\frac{dv}{dt} < 0$ and thus the disease-free equilibrium will be globally asymptotically stable.

3.10.1.2 Endemic Equilibrium Points

The endemic equilibrium E_1 can be computed by setting the right-hand side of the equation (3.1) to zero. Upon solving, we have:

$$E_1 = [S^*, I^*, T^*, V^*, D^*].$$

where

$$\begin{aligned}
S^* &= \frac{\Lambda}{\lambda + \mu}, \\
I^* &= \frac{\lambda \Lambda}{(\lambda + \mu)(\delta + \theta_1 + \mu)}, \\
T^* &= \frac{\theta_1 \lambda \Lambda (\delta + \theta_3 + \mu)(\theta_2 \psi_c + \mu)}{\Omega}, \\
V^* &= -\frac{\theta_1 \lambda \Lambda (\kappa \psi_c - \kappa)(\delta + \theta_3 + \mu)}{\Omega}, \text{ and} \\
D^* &= \frac{\theta_1 \lambda \Lambda (-\theta_2 \kappa \psi_c^2 + \theta_2 \kappa \psi_c + \theta_2 \mu \psi_c + \theta_2^2 \psi_c^2)}{\Omega}.
\end{aligned} \tag{3.59}$$

where:

$$\begin{aligned}
\Omega &= (\lambda + \mu)(\delta + \theta_1 + \mu)(\delta^2 \theta_2 \psi_c + \delta^2 \mu - \delta \theta_2 \kappa \psi_c^2 + \delta \theta_2 \kappa \psi_c \\
&\quad + \delta \theta_2^2 \psi_c^2 + \delta \theta_2 \theta_3 \psi_c - \delta \kappa \mu \psi_c + \delta \kappa \mu + 2\delta \mu^2 - \theta_2 \kappa \mu \psi_c^2 \\
&\quad - \theta_3 \kappa \mu \psi_c + \theta_3 \kappa \mu + 2\theta_2 \mu^2 \psi_c + \theta_3 \mu^2 + \theta_2^2 \mu \psi_c^2 + \theta_2 \theta_3 \mu \psi_c \\
&\quad - \kappa \mu^2 \psi_c + \kappa \mu^2 + \mu^3 + \delta \theta_3 \mu + 3\delta \theta_2 \mu \psi_c + \theta_2 \kappa \mu \psi_c).
\end{aligned}$$



Chapter 4

Sensitivity Analysis and Numerical Simulations

4.1 Introduction

In this chapter, we generate the forward sensitivity indices and perform numerical simulations in Matlab, using the parameter values provided in Table (3.2) These methods are used to validate the analytical results presented in the previous subsections. In addition, numerical simulations of the HIV-culture model (3.1) are conducted to evaluate the impact of cultural practices on the transmission dynamic of HIV.

4.1.1 Sensitivity Analysis

In Mathematical modeling, sensitivity analysis is used to assess the extent to which various parameters affect the model outputs. The sensitivity analysis of the model parameters is done using the normalized forward sensitivity index. This determines how different parameters affect the disease reproduction number, R_v . The sensitivity index for a parameter denoted I is given as:

$$I_s = \frac{\partial R_v}{\partial s} \times \frac{s}{R_v}. \quad (4.1)$$

where,

$$R_v = \frac{\beta \pi_0 (1 - \psi_m) (1 - (1 - \alpha_i) (1 - \alpha_p) (1 - \alpha_w))}{(\theta_1 + \mu + \delta)}. \quad (4.2)$$

For instance the sensitivity index for β is given by

$$I_{\beta} = \frac{\partial R_v}{\partial \beta} \times \frac{\beta}{R_v} = +1 \quad (4.3)$$

similarly;

$$I_{\pi_o} = \frac{\partial R_v}{\partial \pi_o} \times \frac{\pi_o}{R_v} = +1, I_{\psi_m} = \frac{\partial R_v}{\partial \pi_m} \times \frac{\pi_m}{R_v} = -\frac{\psi_m}{1 - \psi_m}, \quad (4.4)$$

$$I_{\theta_1} = \frac{\partial R_v}{\partial \theta_1} \times \frac{\theta_1}{R_v} = -\frac{\theta_1}{\delta + \theta_1 + \mu}, I_{\mu} = \frac{\partial R_v}{\partial \mu} \times \frac{\mu}{R_v} = -\frac{\mu}{\delta + \theta_1 + \mu}, \quad (4.5)$$

$$I_{\delta} = \frac{\partial R_v}{\partial \delta} \times \frac{\delta}{R_v} = -\frac{\delta}{\delta + \theta_1 + \mu}, I_{\alpha_i} = \frac{\partial R_v}{\partial \alpha_i} \times \frac{\alpha_i}{R_v} = \frac{\alpha_i (1 - \alpha_p) (1 - \alpha_w)}{1 - (1 - \alpha_i) (1 - \alpha_p) (1 - \alpha_w)}, \quad (4.6)$$

$$I_{\alpha_p} = \frac{\partial R_v}{\partial \alpha_p} \times \frac{\alpha_p}{R_v} = \frac{\alpha_p (1 - \alpha_i) (1 - \alpha_w)}{1 - (1 - \alpha_i) (1 - \alpha_p) (1 - \alpha_w)}, I_{\alpha_w} = \frac{\partial R_v}{\partial \alpha_w} \times \frac{\alpha_w}{R_v} = \frac{\alpha_w (1 - \alpha_i) (1 - \alpha_p)}{1 - (1 - \alpha_i) (1 - \alpha_p) (1 - \alpha_w)}. \quad (4.7)$$

Using the parameter values in Table 3.2 we obtain the sensitivity indices given in Table 4.1.

The sensitivity indices in this study provided valuable insight into the relative importance of various parameters influencing the dynamics of HIV transmission. The parameter with the highest sensitivity index was identified as the most impactful. As shown in Table 4.1, the infection rate and the cultural practices (α_i , α_p , and α_w) have a significant impact on the reproduction number R_v . A high sensitivity index signifies that a parameter is a key driver of transmission, meaning that small changes in such parameters can lead to large changes in the reproduction number. This has important programmatic implications. A high sensitivity index signifies that a parameter is a key driver of transmission and thus a potential target for effective intervention. For example, interventions that reduce the impact of risky cultural practices (reflected in α_i , α_p , and α_w) could yield meaningful reductions in new infections. Conversely, parameters with low sensitivity indices have limited effect on the model's outcome, and focusing on them may not lead to substantial epidemiological benefits. The results indicate that β and π_o are the most sensitive parameters. However, these parameters were not varied in the simulations, as the primary focus was on the effect of cultural practices.

Table 4.1: Sensitivity Analysis of Parameters.

Parameter	Sensitivity Index
β	1.00000
θ_1	-0.28533
ψ_m	-1.00000
π_o	1.00000
α_p	0.61138
α_i	0.57736
α_w	0.48242
δ	-0.47700
μ	-0.23767

4.1.2 Numerical Simulations

The parameter values used in the numerical simulations of the system (3.1) are presented in Table 3.2. The mathematical study of the effect of cultural practices on the transmission dynamics of HIV is still in its early stages; therefore, many parameter values in Table 3.2 are reasonably assumed. For this study, the population of Luo-Nyanza region is assumed to be 4,397,143, based on the 2019 Kenya Population and Housing Census Results (Kenya National Bureau of Statistics, 2019).

Numerical simulations were performed using Matlab Software whereby different level of cultural influence were evaluated with low cultural influence ranged from 0.10–0.30, moderate cultural influence ranged from 0.35–0.55, and high cultural influence ranged from 0.60–0.90. The following data from the NSDCC 2018 report ? were used as initial conditions:

$$N_0 = [S, I, T, V, D] = [3332150, 433632, 348147, 280694, 24525].$$

Also, the model was analyzed numerically using the parameter values outlined in Table 3.2. The objective was to evaluate the model solutions and explore the potential effects of parameter changes on HIV transmission dynamics. Based on the parameters in Table 3.2, the effective reproduction number was calculated as $R_v = 3.36304$, indicating that the disease will persist in the population.

4.1.3 Effect of Cultural Practices on the Effective Reproduction Number

The resulting curve shown in Figure (4.1) demonstrates the relationship between the influence of cultural practices (ψ_c) and the effective reproduction number (R_v), which quantifies the potential for disease transmission within the population. As the curve shows, there is a positive correlation between the prevalence of cultural practices and the increase in R_v . This means that as these cultural practices become more prevalent, the risk of disease transmission also rises. The curve exhibits a steep initial rise for lower values of ψ_c , indicating that even modest increases in cultural practices lead to a significant rise in R_v . In the Figure (4.1) the value for cultural practices 0.1 imply that there is a low influence of cultural practices while 1 indicates a very high influence of cultural practices.

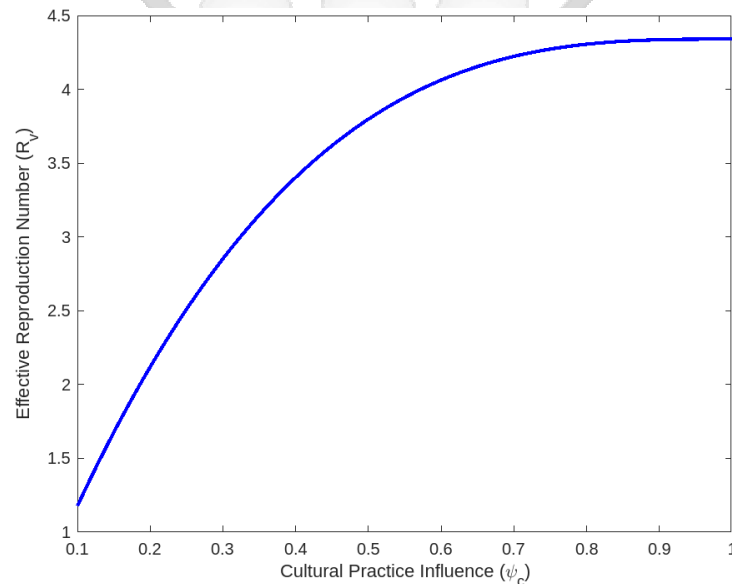


Figure 4.1: A graph showing the effect of cultural practices on the reproduction number

Notably, the curve does not begin at zero, which aligns with the assumption that cultural practices are a constant aspect of social life and will never be entirely absent. These practices, such as wife inheritance, polygamy, and widow cleansing, are hypothesized to contribute significantly to sustaining higher rates of HIV transmission. The findings underscore the importance of culturally sensitive public health interventions, as these practices help keep R_v above the critical threshold needed for continued transmission of the disease. Therefore, any efforts to reduce the transmission of HIV in this population should consider culturally tailored intervention to lower R_v effectively.

4.1.3.1 Effect of Cultural Practices on HIV Infection Dynamics

The graph in Figure 4.2 illustrates the impact of cultural practices on HIV transmission in the Luo-Nyanza region, showing a direct correlation between the level of cultural influence and the rate of infection. In the high cultural influence scenario, HIV transmission is most pronounced, with a sharp and early peak in infections. This trend is largely attributed to deeply ingrained cultural norms such as widow cleansing, wife inheritance, and polygamy, which continue to play a critical role in sustaining the epidemic. Widow cleansing, in particular, involves unprotected intercourse as part of traditional mourning rituals, significantly increasing transmission risks, especially if the deceased had succumbed to HIV/AIDS-related complications. Similarly, wife inheritance without mandatory HIV testing further facilitates the spread of HIV within communities.

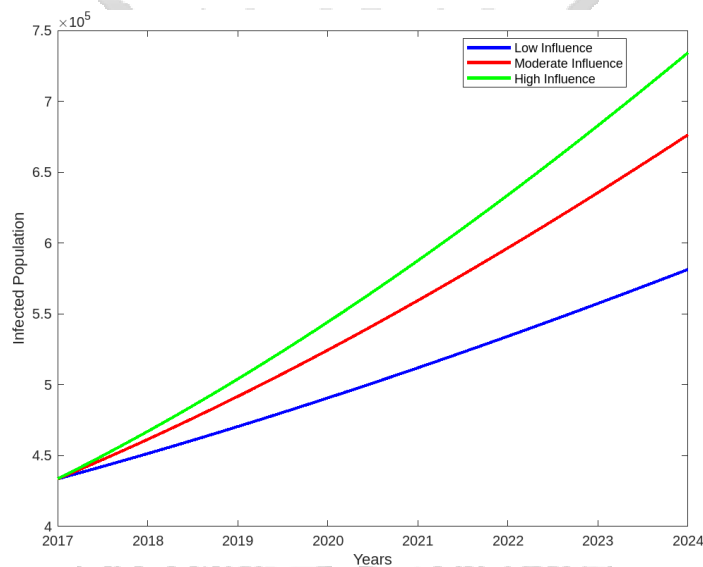


Figure 4.2: A graph showing the effect of cultural practices on HIV infection dynamics at Low Cultural Influence: 0.1–0.3, Moderate Cultural Influence: 0.35–0.55, High Cultural Influence: 0.60–0.90.

The moderate influence scenario reflects a similar but slower rate of infection growth, indicating that while cultural factors still contribute to transmission, certain mitigating factors such as increased awareness, gradual shifts in practices, and targeted intervention programs help slow down the epidemic's progression. In contrast, the low influence scenario represents a more controlled rise in infections, where cultural norms exert minimal impact on disease spread. Here, factors such as early testing and treatment and reduced adherence to high-risk traditional practices play a crucial role in limiting transmission. However, the findings suggest that even in lower-influence settings, cultural

norms cannot be entirely ignored, as they still shape health-seeking behavior and attitudes toward HIV prevention.

These findings in this study align with previous research by [Magadi et al. \(2021\)](#), who highlighted the role of cultural practices in shaping HIV risk behavior in communities with strong traditional norms. The mathematical model in this study confirms these observations by quantifying how cultural influence impacts transmission rates.

4.1.3.2 Effect of Cultural Practices on Retention to Treatment

The graph in [Figure 4.3](#) illustrates the impact of cultural practices on ART dropout rates over time, emphasizing how deeply entrenched practices shape treatment retention. When cultural influence is high, dropout rates rise rapidly, peaking earlier and at a significantly higher level than in other scenarios. This suggests that practices such as widow cleansing, wife inheritance, and polygamy create substantial barriers to treatment adherence, pushing individuals out of care more quickly. In such settings, societal pressures discourage consistent ART use.

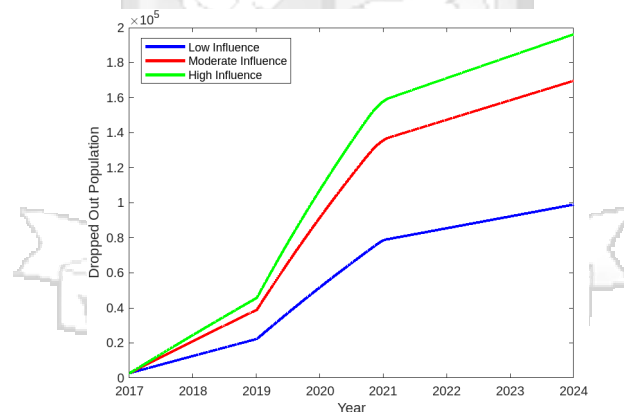


Figure 4.3: A graph showing the effect of cultural practices on retention to Treatment at Low cultural influence: 0.1–0.3, Moderate Cultural Influence: 0.35–0.55, High Cultural Influence: 0.60–0.90.

Under moderate cultural influence, dropout rates still increase but at a slower pace, with the peak occurring later and at a lower magnitude than in high-influence settings. This indicates that while cultural expectations still affect ART adherence, they do not exert an overwhelming force. Individual engaging in risky cultural practices at such a level may experience some level of autonomy in seeking healthcare, but these practices remain a significant challenge to retention.

When cultural influence is minimal, dropout rates are the lowest. This pattern suggests that in environments with fewer influence of culture, individuals are more likely to remain in treatment, benefiting from consistent access to ART. The lower dropout rates in such settings highlight the importance of reducing cultural stigma and providing support systems that reinforce treatment adherence.

A notable exception in the trend appears between 2019 and 2021, where dropout rates surge across all scenarios. This sharp increase coincides with the COVID-19 pandemic, which disrupted healthcare access, increased economic hardships, and instilled fear of visiting health facilities. For individuals in culturally entrenched settings, the pandemic further exacerbated the pre-existing challenges, as movement restrictions and healthcare disruptions made ART refills and routine monitoring even harder to maintain. In these communities, where reliance on traditional healing practices and stigma surrounding ART is already prevalent, the pandemic likely intensified dropout rates beyond what cultural barriers alone would have caused.

Overall, the graph underscores the interplay between cultural norms and external disruptions in shaping ART dropout rates. While cultural practices fundamentally dictate long-term trends, external shocks like COVID-19 can accelerate dropout rates even in lower-influence scenarios. Addressing these challenges requires culturally sensitive interventions that not only tackle harmful traditional norms but also reinforce treatment continuity during crises.

4.1.3.3 Effect of Cultural Practices on Viral Load Suppression

Figure 4.4 illustrates the effect of cultural influence on the viral load-suppressed population over time, revealing a clear inverse relationship: as cultural influence increases, the ability to maintain viral suppression diminishes, leading to a faster decline in the suppressed population. This trend highlights the significant role that cultural practices play in shaping HIV treatment adherence and long-term health outcomes.

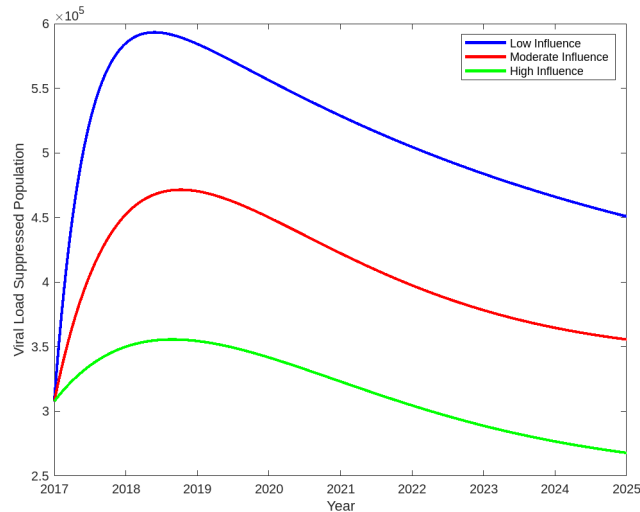


Figure 4.4: A graph showing the effect of cultural practices on viral load suppression at Low cultural influence: 0.1–0.3, Moderate Cultural Influence: 0.35–0.55, High Cultural Influence: 0.60–0.90.

In settings with low cultural influence, the viral load-suppressed population remains consistently high, indicating minimal interference with treatment adherence. This suggests that when cultural barriers are minimal, individuals are more likely to stay on antiretroviral therapy (ART) and achieve sustained viral suppression. In contrast, the moderate-influence scenario shows a more noticeable decline, implying that cultural norms and beliefs moderately disrupt treatment retention and intervention effectiveness. The high-influence scenario exhibits the steepest and most sustained drop in viral suppression, suggesting that deeply ingrained cultural practices significantly hinder individuals' willingness and ability to adhere to ART.

A particularly sharp decline in viral suppression is observed between 2019 and 2021 across all influence levels, coinciding with the COVID-19 pandemic. The pandemic disrupted healthcare access globally, restricting movement, limiting ART refills, and reducing routine viral load monitoring. Fear of contracting COVID-19 at health facilities further discouraged individuals from seeking care. In culturally entrenched settings, reliance on traditional healing methods and persistent stigma surrounding ART may have exacerbated these disruptions, prolonging the period of low viral suppression.

Within the Luo-Nyanza region, cultural practices such as widow cleansing, wife inheritance, and polygamy further shape HIV treatment outcomes. These practices often create additional barriers to ART adherence by reinforcing stigma and restricting access to care. Without targeted interventions

that address these risky cultural practices, achieving and maintaining viral suppression in such communities remains difficult.

4.1.3.4 Effect of Cultural Practices on ART Treatment

The graph in figure 4.5 illustrates the trajectory of the treatment population under different cultural influence scenarios—low, moderate, and high. At the start of the observation period, all three scenarios begin with nearly identical treatment populations. However, as time progresses, a divergence emerges, reflecting the impact of cultural practices on both infection rates and treatment adherence.

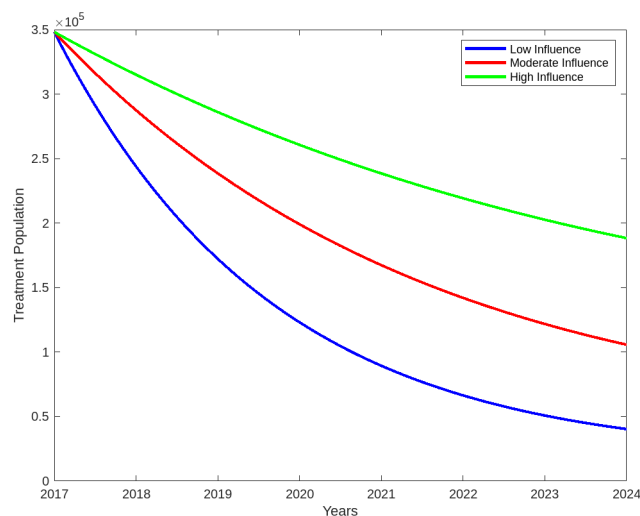


Figure 4.5: A graph showing the effect of cultural practices on ART treatment at Low cultural influence: 0.1–0.3, Moderate Cultural Influence: 0.35–0.55, High Cultural Influence: 0.60–0.90.

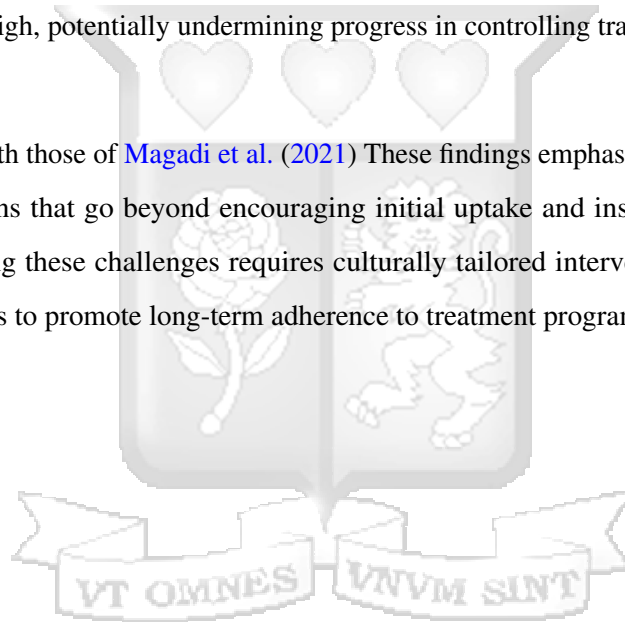
In the high influence scenario (green curve), the initial treatment population remains higher than in the moderate (red) and low (blue) influence cases. This can be attributed to the fact that in communities with stronger cultural practices, more individuals are expected to be infected, leading to a higher number of people seeking treatment. However, despite this initial advantage, the treatment population gradually declines over time. This decline is driven by dropout rates, influenced by factors such as indulging in risky cultural practice and possible disruptions like the COVID-19 pandemic.

The moderate influence scenario (red curve) follows a similar downward trajectory, but at a slightly steeper rate compared to the high influence group. This suggests that while infection rates and treatment entry remain significant, fewer individuals are enrolled in care, and dropout rates contribute

steadily to the decrease in treatment retention. The low influence scenario (blue curve) exhibits the sharpest decline, starting from the smallest initial treatment population. In these communities, fewer individuals are exposed to infection due to lower cultural influences facilitating transmission. Consequently, fewer people require treatment in the first place. However, those who do enter treatment still face challenges in maintaining adherence, leading to a steady drop in numbers over time.

Overall, the graph underscores a critical pattern: while stronger cultural influences lead to higher initial treatment populations due to increased infection rates, long-term retention remains a challenge across all scenarios. The downward trends highlight the need for sustained interventions, such as improving healthcare access, strengthening community-based support systems, and addressing social determinants that affect treatment adherence. Without these efforts, the risk of individuals dropping out of care remains high, potentially undermining progress in controlling transmission and improving health outcomes.

The findings align with those of [Magadi et al. \(2021\)](#) These findings emphasize the need for culturally sensitive interventions that go beyond encouraging initial uptake and instead focus on long-term retention. Addressing these challenges requires culturally tailored interventions that work within community structures to promote long-term adherence to treatment programs.



Chapter 5

Conclusion and Recommendation

In this study, a population-based mathematical model was developed to assess the impact of cultural practices on HIV transmission dynamics in Luo-Nyanza. The model was evaluated for positivity and boundedness to ensure well-posedness, and the effective reproduction number (R_v) was derived using the next-generation matrix approach. Stability analysis showed that when R_v is below unity, the disease-free equilibrium (DFE) is locally stable, confirming that controlling the influence of cultural practices can help curb transmission. The global stability of the DFE was further verified using the Lyapunov function, confirming that under appropriate intervention strategies, the epidemic can be controlled. Numerical simulations revealed that high-risk cultural practices significantly accelerate HIV transmission, reinforcing the urgent need for culturally tailored interventions that align with community norms rather than attempting to eliminate these practices entirely which may not be practically feasible.

The findings highlight that deep-rooted cultural traditions serve as a persistent barrier to HIV prevention, treatment adherence, retention in care, and viral load suppression. Practices such as widow cleansing and wife inheritance perpetuate unprotected sexual encounters, increasing the likelihood of reinfection, while polygamy amplifies transmission by expanding sexual networks where prevention measures remain inconsistent. The study also establishes that the degree of cultural influence directly correlates with the severity of the epidemic, with higher influence leading to a more pronounced impact on transmission rates. However, even in low-influence scenarios, cultural practices continue to shape HIV dynamics, underscoring the importance of strategies that engage communities rather than oppose their traditions. These results align with prior studies, including that of [Agot et al. \(2010\)](#) and [Magadi et al. \(2021\)](#), which identified cultural practices as key contributors to HIV persistence in the Luo-Nyanza region of Western Kenya.

5.1 Recommendation

To effectively address the impact of cultural practices on HIV transmission in Luo-Nyanza, interventions must be designed to work within cultural contexts rather than against them. Since eliminating these practices may not be feasible, interventions should focus on ways to be sensitive to community beliefs while promoting safer behavior. Thus, programs and interventions aimed at reducing HIV transmission should be tailored to incorporate culturally sensitive interventions in a way that mitigates the risk of cultural practices. For instance, safe alternatives to practices like widow cleansing can be introduced, offering culturally acceptable methods that reduce the likelihood of HIV spread. Additionally, engaging community elders, integrating HIV education into traditional gatherings and collaborating with cultural leaders to shift harmful norms can foster greater acceptance and effectiveness. By aligning HIV interventions with the cultural realities of the Luo-Nyanza region, public health efforts can be more effective, ensuring that they resonate with the population while achieving the goal of reducing transmission.

5.2 Future Research

While this study provides significant insights into the role of cultural practices in shaping HIV transmission dynamics in Luo-Nyanza, several limitations present opportunities for further research. Addressing these gaps will enhance the effectiveness of culturally tailored interventions and improve public health outcomes.

1. Comparison of the Effect of Individual Practices: More research is required to ascertain which cultural practices have the highest impact on HIV transmission dynamics in the region
2. Effectiveness of Culturally Tailored Interventions: While this study highlights the need for culturally sensitive approaches it does not evaluate the effectiveness of the culturally sensitive interventions, further research should evaluate the impact of these specific interventions
3. Development of a Sex-Structured HIV Transmission Model: This study assumes a homogeneous population, but given the significant biological and behavioral differences between men and women in HIV transmission and treatment adherence, future research should develop a

sex-structured mathematical model. Such a model would help quantify how engaging in these cultural practices impact HIV transmission differently for men and women.

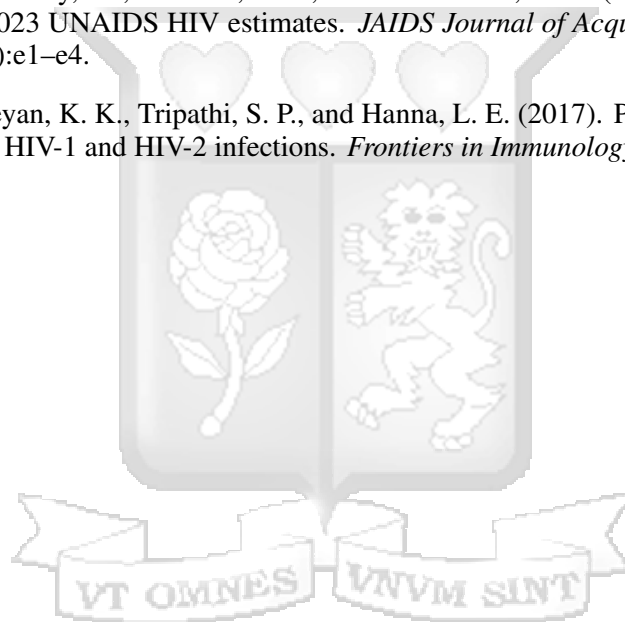
By addressing these research gaps, future studies can enhance the effectiveness of HIV interventions in culturally rich settings like Luo-Nyanza, ensuring that public health strategies are both scientifically sound and socially acceptable.



References

- Agot, K. E., Vander Stoep, A., Tracy, M., Obare, B. A., Bukusi, E. A., Ndinya-Achola, J. O., Moses, S., and Weiss, N. S. (2010). Widow inheritance and HIV prevalence in Bondo District, Kenya: baseline results from a prospective cohort study. *PloS one*, 5(11):e14028.
- Ayikukwei, R., Ngare, D., Sidle, J., Ayuku, D., Baliddawa, J., and Greene, J. (2008). HIV/AIDS and cultural practices in western Kenya: the impact of sexual cleansing rituals on sexual behaviours. *Culture, Health & Sexuality*, 10(6):587–599.
- Bozkurt, F. and Peker, F. (2014). Mathematical modelling of HIV epidemic and stability analysis. *Advances in Difference Equations*, 2014:1–17.
- Cassels, S., Clark, S. J., and Morris, M. (2008). Mathematical models for HIV transmission dynamics: tools for social and behavioral science research. *JAIDS Journal of Acquired Immune Deficiency Syndromes*, 47:S34–S39.
- Diekmann, O., Heesterbeek, J. A. P., and Metz, J. A. J. (1990). On the definition and the computation of the basic reproduction ratio R_0 in models for infectious diseases in heterogeneous populations. *Journal of mathematical biology*, 28:365–382.
- Gelmon, L. (2009). Kenya HIV Prevention Response and Modes of Transmission Analysis. Final Report. Kenya National AIDS Control Council. <https://documents1.worldbank.org/curated/en/229521468331880313/pdf/483560SR0P1113101same0box101PUBLIC1.pdf>.
- Huo, H.-F., Chen, R., and Wang, X.-Y. (2016). Modelling and stability of HIV/AIDS epidemic model with treatment. *Applied Mathematical Modelling*, 40(13-14):6550–6559.
- Kenya Ministry of Health, N. (2020). Kenya Population-based HIV Impact Assessment (KENPHIA) 2018: Final Report. https://phia.icap.columbia.edu/wp-content/uploads/2022/08/KENPHIA_Ago25-DIGITAL.pdf. 2025-01-10.
- Kenya National Bureau of Statistics (2019). The 2009 Kenya Population and Housing Census. <https://www.knbs.or.ke/wp-content/uploads/2023/09/2009-Kenya-population-and-Housing-Census-Analytical-Report-on-Kenya-Population-Atlas.pdf>. [Accessed:2024-10-04].
- Kharsany, A. B. and Karim, Q. A. (2016). HIV infection and AIDS in Sub-Saharan Africa: current status, challenges and opportunities. *The open AIDS journal*, 10:34.
- Magadi, M., Gazimbi, M., Wafula, C., and Kaseje, M. (2021). Understanding ethnic variations in HIV prevalence in Kenya: The role of cultural practices. *Culture, Health & Sexuality*, 23(6):822–839.
- Munala, L., Harris, M., and Mwangi, E. (2019). Submit to Survive: An exploration of sexual cleansing as an act of violence against widows in the Luo of Kenya. *Culture, Health & Sexuality*, 25(6):698–710.
- Mwangi, S. M. N., Kitetu, V. M., and Okwany, I. O. (2024). Mathematical Modeling of HIV Investigating the Effect of Inconsistent Treatment. *Journal of Applied Mathematics and Physics*, 12(4):1063–1078.
- Ngina, P., Mbogo, R. W., and Luboobi, L. S. (2017). The In Vivo Dynamics of HIV Infection with the Influence of Cytotoxic T Lymphocyte Cells. *International Scholarly Research Notices*, 2017(1):2124789.

- Nhendo, C. (2019). A mathematical model of HIV/AIDS population dynamics with treatment failure and treatment dropouts in the era of universal test and treat approach. PhD thesis, Midlands State University.
- NSDCC (2022). World AIDS Day Report 2022. https://nsdcc.go.ke/wp-content/uploads/2022/12/WAD-Report_f4_print.pdf. Accessed: [2024-09-04].
- NSDCC (2023). Kenya County HIV Estimates. <https://analytics.nsdcc.go.ke/estimates/#!/kenya/countywkbook>. Accessed: [2024-09-05].
- Udofia, E. S. (2023). Mathematical model of male circumcision in HIV/AIDS preventions. *International Journal of Innovative Science and Research Technology*, 8(8).
- Van den Driessche, P. and Watmough, J. (2002). Reproduction numbers and sub-threshold endemic equilibria for compartmental models of disease transmission. *Mathematical biosciences*, 180(1-2):29–48.
- Van Schalkwyk, C., Mahy, M., Johnson, L. F., and Imai-Eaton, J. W. (2024). Updated data and methods for the 2023 UNAIDS HIV estimates. *JAIDS Journal of Acquired Immune Deficiency Syndromes*, 95(1S):e1–e4.
- Vijayan, V., Karthigeyan, K. K., Tripathi, S. P., and Hanna, L. E. (2017). Pathophysiology of CD4+ T-cell depletion in HIV-1 and HIV-2 infections. *Frontiers in Immunology*, 8:580.



Appendices

Appendix A: Similarity Report

A Mathematical Model on the Effect of Cultural Practices on HIV Transmission Dynamics in Western Kenya-167902.pdf

ORIGINALITY REPORT

12%

SIMILARITY INDEX

9%

INTERNET SOURCES

9%

PUBLICATIONS

8%

STUDENT PAPERS

PRIMARY SOURCES

1

Submitted to Strathmore University

Student Paper

4%

2

su-plus.strathmore.edu

Internet Source

4%

3

researchspace.ukzn.ac.za

Internet Source

<1%

4

Ranjit Kumar Upadhyay, Satteluri R. K. Iyengar. "Spatial Dynamics and Pattern Formation in Biological Populations", CRC Press, 2021

Publication

<1%

5

uir.unisa.ac.za

Internet Source

<1%

6

S. Bahloul,, Bothina Shahin, H. Kabeel. "EFFECT OF SOME CULTURAL PRACTICES ON FLOWER BUD FORMATION, FRUIT SET AND YIELD OF 'LE-CONTE" PEAR TREES", Journal of Plant Production, 2000

Publication

<1%

7	Submitted to The African Institute for Mathematical Sciences Student Paper	<1%
8	dspace.nm-aist.ac.tz Internet Source	<1%
9	nsdcc.go.ke Internet Source	<1%
10	Submitted to Universiteit van Amsterdam Student Paper	<1%
11	edocs.maseno.ac.ke Internet Source	<1%
12	dione.lib.unipi.gr Internet Source	<1%
13	S. B. Chibaya, F. Nyabadza. "Mathematical Modelling of the Potential Role of Supplementary Feeding for People Living with HIV/AIDS", International Journal of Applied and Computational Mathematics, 2019 Publication	<1%
14	Submitted to University of Zululand Student Paper	<1%
15	Hai-Feng Huo, Rui Chen, Xun-Yang Wang. "Modelling and stability of HIV/AIDS epidemic model with treatment", Applied Mathematical Modelling, 2016 Publication	<1%

Appendix B: Ethical Clearance Confirmation



Strathmore
UNIVERSITY

17th December 2024

Ms Lago Sally,
sally.stellah@strathmore.edu

Dear Ms Lago,

RE: A Mathematical Model on the Effect of Cultural Practices on HIV Transmission Dynamics in Western Kenya

This is to inform you that SU-ISERC has reviewed and **approved** your above **SU-masters** proposal. Your application reference number is **SU-ISERC2450/24**. The approval period is from **17th December 2024 to 16th December 2025**.

This approval is subject to compliance with the following requirements:

- i. Only approved documents including (informed consents, study instruments, MTA) will be used.
- ii. All changes including (amendments, deviations, and violations) are submitted for review and approval by SU-ISERC.
- iii. Death and life-threatening problems and serious adverse events or unexpected adverse events whether related or unrelated to the study must be reported to SU-ISERC within 72 hours of notification.
- iv. Any changes anticipated or otherwise that may increase the risks or affected safety or welfare of study participants and others or affect the integrity of the research must be reported to SU-ISERC within 72 hours.
- v. Clearance for the export of biological specimens must be obtained from relevant institutions.
- vi. Submission of a request for renewal of approval at least 60 days prior to the expiry of the approval period. Attach a comprehensive progress report to support the renewal.
- vii. Submission of an executive summary report within 90 days of completion of the study to SU-ISERC.

Before commencing your study, you will be expected to obtain a research license from National Commission for Science, Technology, and Innovation (NACOSTI) <https://research-portal.nacosti.go.ke/> and obtain other clearances needed.

Yours sincerely,

A handwritten signature in black ink, appearing to read 'Ambrose Rachier'.

Mr Ambrose Rachier,
Chairperson; SU-ISERC

Appendix C: Runge-Kutta Fourth Order Outline

The formula for the fourth-order Runge-Kutta method is given by:

$$y_{n+1} = y_n + \frac{h}{6}(k_1 + 2k_2 + 2k_3 + k_4) \quad (1)$$

where the slope estimates k_1 , k_2 , k_3 , and k_4 are calculated as follows:

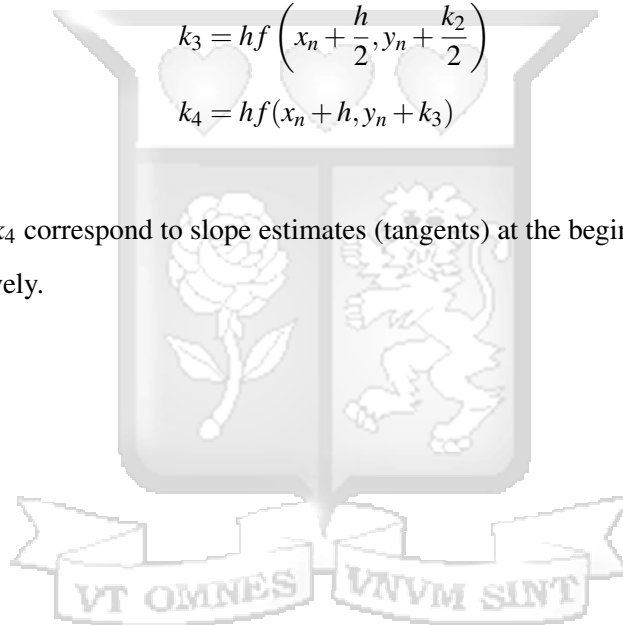
$$k_1 = hf(x_n, y_n) \quad (2)$$

$$k_2 = hf\left(x_n + \frac{h}{2}, y_n + \frac{k_1}{2}\right) \quad (3)$$

$$k_3 = hf\left(x_n + \frac{h}{2}, y_n + \frac{k_2}{2}\right) \quad (4)$$

$$k_4 = hf(x_n + h, y_n + k_3) \quad (5)$$

Here, k_1 , k_2 , k_3 , and k_4 correspond to slope estimates (tangents) at the beginning, middle, and end of the interval, respectively.



Appendix D: Matlab Codes

```
1 % Define the parameters
2 Lambda = 0.2754;          % Recruitment rate of susceptible
    individuals: World Bank Estimate 2022
3 beta = 0.13;             % Rate of infection in Nyanza:
    NSDCC report 2023
4 psi_m = 0.5;             % Reduction in transmission rate
    due to circumcision: KENPHIA report
5 pi_0 = 2.2;              % Infectiousness of individuals in
    I(t): Assumed
6 pi_1 = 1.8;              % Infectiousness of individuals in
    D(t): Assumed
7 theta_1 = 0.0094;        % Rate of treatment enrollment:
    National Syndemic Diseases Control Council, Kenya HIV
    Estimates 2024
8 theta_2 = 0.039;         % Rate of dropping out of treatment
    : :National Syndemic Diseases Control Council, Kenya HIV
    Estimates 2024
9 theta_3 = 0.00902;       % Rate of reinitiation to treatment
    :Nhendo
10 kappa = 0.906;          % ART adherence rate
11 mu = 0.00783;           % Natural death rate:World Bank
12 delta = 0.015714286;    % Disease-induced death rate:NACC
    estimates 2021
13
14 % Define initial conditions
15 S0 = 3246511;           % Initial susceptible population
16 I0 = 444707;            % Initial infected population
17 T0 = 377652;            % Initial treated population
```

```

18 V0 = 307861;           % Initial population with
    suppressed viral load
19 D0 = 10206;           % Initial drop-out population
20 N0 = S0 + I0 + T0 + V0 + D0; % Initial total population
21
22 % Define the time span for the simulation
23 tspan = [2017:0.0005:2024];
24
25 %tspan=linspace(0,30,length(years));
26 % Define cultural practice scenarios: low, moderate, and
    high
27 cultural_scenarios = [
28
29     0.23, 0.24, 0.20; % Low Cultural Influence(alpha
    values)
30     0.37, 0.30, 0.45; % Moderate Cultural Influence
31     0.65, 0.8, 0.75; % High Cultural Influence
32
33 ];
34
35 % Predefine names and colors for each scenario
36 scenario_names = {'Low Influence', 'Moderate Influence', '
    High Influence'};
37 colors = ['b', 'r', 'g'];
38 %;,J H
39 % Loop over cultural scenarios
40 for i = 1:size(cultural_scenarios, 1)
41     % Extract cultural impact parameters for the current
    scenario
42     alpha_p = cultural_scenarios(i, 1);

```

```

43     alpha_w = cultural_scenarios(i, 2);
44     alpha_i = cultural_scenarios(i, 3);
45
46     % Compute psi_c for the current scenario
47     psi_c = 1 - ((1 - alpha_p) * (1 - alpha_w) * (1 -
         alpha_i));
48
49     % Solve the system of differential equations using
         ode45
50     [t, X] = ode45(@(t, X) modelEquations(t, X, Lambda,
         beta, psi_m, psi_c, pi_0, pi_1, theta_1, theta_2,
         theta_3, kappa, mu, delta), tspan, [S0, I0, T0, V0,
         D0]);
51
52     % Extract the results
53     S = X(:, 1);
54     I = X(:, 2);
55     T = X(:, 3);
56     V = X(:, 4);
57     D = X(:, 5);
58
59     % Plot the results for each population
60     figure(1); % Susceptible population
61     plot(t, S, colors(i), 'DisplayName', scenario_names{i},
         'LineWidth', 2); hold on;
62
63     figure(2); % Infected population
64     plot(t, I, colors(i), 'DisplayName', scenario_names{i},
         'LineWidth', 2); hold on;
65

```

```

66     figure(3); % Treated population
67     plot(t, T, colors(i), 'DisplayName', scenario_names{i},
          'LineWidth', 2); hold on;
68
69     figure(4); % Viral Load Suppressed population
70     plot(t, V, colors(i), 'DisplayName', scenario_names{i},
          'LineWidth', 2); hold on;
71
72     figure(5); % Dropped Out population
73     plot(t, D, colors(i), 'DisplayName', scenario_names{i},
          'LineWidth', 2); hold on;
74 end
75
76 % Add legends and labels to each figure
77 for fig = 1:5
78     figure(fig);
79     xlabel('Time(days)');
80     switch fig
81     case 1
82         ylabel('Susceptible Population');
83         % title('Susceptible Population Over Time');
84     case 2
85         ylabel('Infected Population');
86         % title('Infected Population Over Time');
87     case 3
88         ylabel('Treatment Population');
89         % title('Treated Population Over Time');
90     case 4
91         ylabel('Viral Load Suppressed Population');

```

```

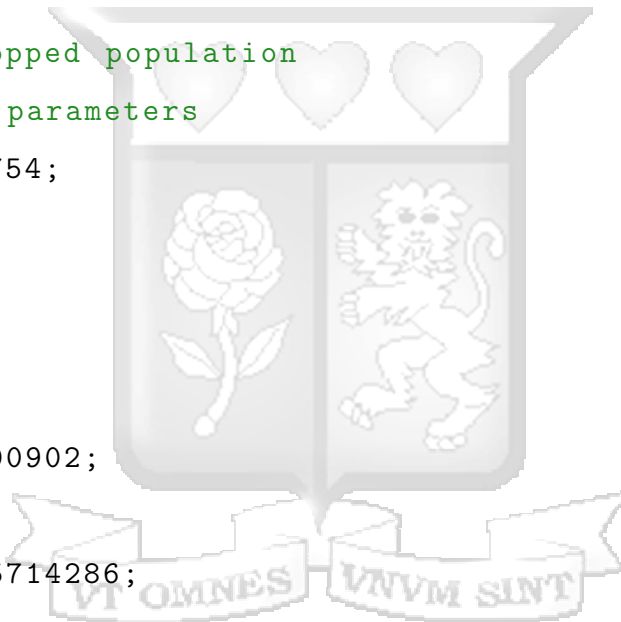
92         % title('Viral Load Suppressed Population Over
           Time');
93     case 5
94         ylabel('Dropped Out Population');
95         %title('Dropped Out Population Over Time');
96     end
97     legend('show');
98     grid on;
99 end
100
101 % Define the system of differential equations as a local
    function
102 function dXdt = modelEquations(t, X, Lambda, beta, psi_m,
    psi_c, pi_0, pi_1, theta_1, theta_2, theta_3, kappa, mu,
    delta)
103     S = X(1);
104     I = X(2);
105     T = X(3);
106     V = X(4);
107     D = X(5);
108     N = S + I + T + V + D; % Total population
109
110     % Force of infection
111     lambda = beta * (psi_c) * (1 - psi_m) * (pi_0 * I +
        pi_1 * D) / ( N);
112
113     % Differential equations
114     dSdt = Lambda - (lambda + mu) * S;
115     dIdt = lambda * S - (theta_1 + mu + delta) * I;

```

```

116     dTdt = theta_1 * I +theta_3*D- (theta_2 * psi_c + kappa
        * (1 - psi_c) + mu + delta) * T;
117     dVdt = kappa * (1 - psi_c) * T - (theta_2 * psi_c + mu)
        * V;
118     dDdt = theta_2 * psi_c * (T + V) - (theta_3 + mu +
        delta) * D;
119
120     dXdt = [dSdt; dIdt; dTdt; dVdt; dDdt];
121 end
122
123 %Plot for dropped population
124 % Define the parameters
125 Lambda = 0.2754;
126 beta = 0.13;
127 psi_m = 0.5;
128 pi_0 = 2.2;
129 pi_1 = 1.8;
130 theta_3 = 0.00902;
131 mu = 0.00783;
132 delta = 0.015714286;
133
134 % Initial conditions
135 S0 = 3246511;
136 I0 = 3217183;
137 T0 = 330396;
138 V0 = 300973;
139 D0 = 2520;
140 N0 = S0 + I0 + T0 + V0 + D0;
141
142 % Time span with finer resolution

```



```

143 tspan = linspace(2017, 2024, 10000);
144
145 % Cultural practice scenarios
146 cultural_scenarios = [
147     0.23, 0.14, 0.1; % Low Influence
148     0.37, 0.30, 0.45; % Moderate Influence
149     0.55, 0.58, 0.5; % High Influence
150 ];
151
152 % Scenario names and colors
153 scenario_names = {'Low Influence', 'Moderate Influence', '
    High Influence'};
154 colors = ['b', 'r', 'g'];
155
156 % Only plot dropped out population (D)
157 figure;
158 hold on;
159
160 for i = 1:size(cultural_scenarios, 1)
161     alpha_p = cultural_scenarios(i, 1);
162     alpha_w = cultural_scenarios(i, 2);
163     alpha_i = cultural_scenarios(i, 3);
164
165     psi_c = 1 - ((1 - alpha_p) * (1 - alpha_w) * (1 -
        alpha_i));
166
167     [t, X] = ode23(@(t, X) modelEquations(t, X, Lambda,
        beta, psi_m, psi_c, pi_0, pi_1, theta_3, mu, delta,
        t), ...
168         tspan, [S0, I0, T0, V0, D0]);

```

```

169
170     D = smoothdata(X(:, 5), 'loess', 30);
171     plot(t, D, colors(i), 'DisplayName', scenario_names{i},
          'LineWidth', 2);
172 end
173
174 xlabel('Year');
175 ylabel('Dropped Out Population');
176 title('Effect of Cultural Influence on Dropout Population
        Over Time');
177 legend('show');
178 grid on;
179
180 % Model equations
181 function dXdt = modelEquations(t, X, Lambda, beta, psi_m,
        psi_c, pi_0, pi_1, theta_3, mu, delta, t_current)
182     S = X(1); I = X(2); T = X(3); V = X(4); D = X(5);
183     N = S + I + T + V + D;
184
185     % COVID period
186     if t_current >= 2019 && t_current <= 2021
187         kappa = 0.3;
188         theta_1 = 0.001;
189         theta_2 = 0.12;
190     else
191         kappa = 0.906;
192         theta_1 = 0.0094;
193         theta_2 = 0.039;
194     end
195

```

```

196     lambda = beta * psi_c * (1 - psi_m) * (pi_0 * I + pi_1
        * D) / N;
197
198     dSdt = Lambda - (lambda + mu) * S;
199     dIdt = lambda * S - (theta_1 + mu + delta) * I;
200     dTdt = theta_1 * I + theta_3 * D - (theta_2 * psi_c +
        kappa * (1 - psi_c) + mu + delta) * T;
201     dVdt = kappa * (1 - psi_c) * T - (theta_2 * psi_c + mu)
        * V;
202     dDdt = theta_2 * psi_c * (T + V) - (theta_3 + mu +
        delta) * D;
203
204     dXdt = [dSdt; dIdt; dTdt; dVdt; dDdt];
205 end
206
207 % Plot R0 against cultural practice influence
208 figure;
209 plot(alpha_values, R0_values, 'b-', 'LineWidth', 2);
210 xlabel('Cultural Practice Influence (\psi_c)');
211 ylabel('Effective Reproduction Number (R_v)');
212 %title('Effect of Cultural Practices on R_v');
213 grid on

```